

Responses to the Comments of the Anonymous Referee #1

We very much appreciate the constructive comments and suggestions from this reviewer. Our point-by-point responses to the reviewer's comments are provided as follows (the reviewer's comments are marked in *Italic font*):

This study tries to quantify the impact of biomass burning (fire) and other anthropogenic (non-fire) sources to the occurrence of low visibility days (LVDs due to PM_{2.5}) in several cities across the Southeast Asia. This is an extension of their work in Lee et al., 2017 by improving the WRF-Chem model components. Regional air quality degradation is assessed using simulated PM_{2.5} and ozone, derived AQI, and mortality calculations. They identify that the inclusion of measured anthropogenic dust component to the model increases performance of the model. They also assessed the performance of some machine learning algorithms to predict the occurrence of LVDs.

Generally, the study is of importance, and relevance to ACP. It can be published with a major revision.

First, the novelty of the work (if any) should be mentioned in the manuscript, in the introduction.

Studies of Southeast Asia air quality using high-resolution models with interactive chemistry and meteorology combining with observations, even for specific cases rather than decadal-scale analysis, are still rare. Our previous study using WRF coupled with a simplified tracer model for PM_{2.5} provided arguably the first such quantitative analysis, which demonstrates that biomass burning aerosols contributed to up to 40-60% of haze events in the major cities of Southeast Asia during 2003-2014 (Lee et al., 2017). In this study, we have further the depth of the analysis by applying a more sophisticated regional weather-chemistry model of WRF-Chem to quantitatively address the impacts of fire and non-fire aerosols on air quality and visibility degradation over Southeast Asia. We have also used available in-situ measurements to evaluate and correct model for providing a better base for further improvement of particularly emissions over the region. Beyond the traditional process models such as WRF-Chem, we have also experimented using machine learning algorithms to identify suitable conditions for hazes based on historical data and hence to forecast the likelihood of the occurrence of such events.

To address the reviewer's point, we have further emphasized the uniqueness of our study in the introduction section of the revised manuscript, by clearly indicating the new methods and approaches adopted in our study.

Authors mention that the underestimation of particulate matter in the model could be due to horizontal resolution or missing anthropogenic dust. Have you considered any other aspects of the model before making such a statement? how about the simulated boundary layer mixing of tracers? why ozone is overestimated in the model?

We have actually used the measured particulate composition data to correct modeled biases due to missing organic matter (residual) besides anthropogenic dust component (Snider et al., 2016) (Fig. S1 in the revised version; also see response to a later comment). Although this was mentioned in the original manuscript, it may have been unclear. We have revised the text accordingly to emphasize the importance of applying the correction to the modeled PM_{2.5} concentration using the measured values of organic matter residuals.

We adopted the Mellor-Yamada-Nakanishi-Niino level 2.5 (MYNN) (Nakanishi and Niino, 2009) as the planetary boundary scheme in this study. The WRF model also has a reasonably fine vertical resolution for the PBL by using a vertical coordinate that is stretched to have higher resolutions inside PBL (e.g., having an average depth of ~30 m near the surface). With four to five model layers within the PBL, the model should be able to reasonably simulate the mixing of tracers in the boundary layer. We have added description of the PBL scheme in the revised manuscript as: “The Mellor-Yamada-Nakanishi-Niino level 2.5 (MYNN) (Nakanishi and Niino, 2009) is chosen as the planetary boundary scheme in this study. By using a vertical coordinate that is stretched to have higher resolutions inside the planetary boundary layer, the model has about 4-5 vertical layers inside the planetary boundary layer with a vertical resolution of ~30 m near the surface.”

We have noticed that NO_x emission is higher in REAS emission inventory compared with other emission inventories and studies (Kurokawa et al., 2013). The boundary condition of background ozone in the default WRF-Chem configuration also appears to be somewhat high (30 ppbv) for our domain. Both could lead to the overestimated ozone in the model. We have added corresponding discussion in Sect. 3.1 in the revised manuscript.

Have you tried the simulations using any other emission inventories? This is very important.

We agree with the reviewer that using different emission inventories in the model would very likely lead to different results as indicated in our previous study (Lee et al., 2017), where we used two different biomass burning inventories in the simulations and derived different results for given cases; however, such differences did not substantially influence our major conclusion. In this study, we have actually compared the differences between the two available emission inventories for WRF-Chem for the targeted domain, the REAS and EDGAR inventories, in a pair of one-year simulations comparing 2006 REAS against EDGAR emissions. The results are shown in Table R1 (Table S3 in revised manuscript). It is quite clear that the differences regarding aerosols are quite limited. After considering the high spatiotemporal resolution of REAS emission inventory and the comparison results, we decided to use REAS in our study. Besides our analysis, Kurokawa et al. (2013) have also documented the comparison of REAS with other emission inventories in Southeast Asia.

In the revised manuscript, we have added that “We have compared the modeled results using REAS versus EDGAR emission inventories in one-year paired simulations: the

differences between these two model runs are rather limited regarding aerosol-related variables (Table S3). After considering high spatiotemporal resolution of REAS emission inventory and the comparison results, we decided to use REAS in this study. In addition, a detail comparison of REAS with other emission inventories in Southeast Asia was also presented by Kurokawa et al. (2013).”

Table R1. Mean annual emissions and modeled concentration of BC, OC, SO₂, CO and NO₂ from 2006 REAS and EDGAR emission inventories in the simulated domain.

	REAS		EDGAR	
	Emissions (Tg/year)	Modeled (ug/m ³ or ppmv)	Emissions (Tg/year)	Modeled (ug/m ³ or ppmv)
OC	0.12	0.1131	0.15	0.1487
BC	0.036	0.0311	0.065	0.0643
SO ₂	0.43	1.03×10 ⁻⁴	0.65	2.01×10 ⁻⁴
NO ₂	0.3	4.94×10 ⁻⁴	0.205	4.83×10 ⁻⁴
CO	3.53	8.10×10 ⁻²	7.48	8.72×10 ⁻²

Model evaluation should be conducted in a much better way before making conclusions. Spatiotemporal distribution of each species should be evaluated thoroughly, in the context of all the modeling components. PM_{2.5} (its components and extinction values) should be assessed, not just PM₁₀ (there are some measurements available).

We appreciate the reviewer’s suggestion. In the revised manuscript, we have modified many presentations of the results in Section 3.1. Nevertheless, a fundamental issue in evaluating model for Southeast Asia domain is the lack of observations. As we described in the manuscript, PM_{2.5} observations in this region are very limited. Even in Singapore, observed PM_{2.5} data are only available after 2014 for the general public and research community to access. In most other Southeast Asian counties, even PM₁₀ measurement data are hard to find, especially for the time periods before 2008. We are fortunate to be able to obtain some chemical species data from WMO and long-term AQI data from the Malaysian government. In addition, PM_{2.5} component data from SPARTAN filtered samples (operated after 2013) have also been used, e.g., in Fig. S1 of the revised version.

Have you assessed the importance of organic matter in PM_{2.5} over these regions? the ‘residual matter’ in Snider et al., 2016 is mainly organic, please refer to that paper; so, the statements such as “including the in situ anthropogenic dust improved the ...” should be revised (since you are adding dust and organics).

We really appreciate the reviewer for raising this issue. Indeed, the residual matters that have actually been used in the study to correct modeled PM_{2.5} concentration are mostly organic carbon, though this was not made clear in the original manuscript. We have made our best effort to clearly indicate this fact in the revised manuscript.

Clearly quantify and describe the uncertainty in your estimates of LVDs etc. (for fire and

non-fire related) derived using model values. An entire section should be devoted to uncertainty analysis.

We appreciate the reviewer’s suggestion. Since a full-scale forward-integrating uncertainty analysis based on WRF-Chem model would extremely expensive computationally, we have adopted a method for dichotomous (yes or no LVDs) cases and then give a contingency table as below to address model evaluation and to quantify model performance.

		Observed LVD	
		yes	no
Modeled LVD	yes	<i>hits</i>	<i>false alarms</i>
	no	<i>misses</i>	<i>correct negatives</i>

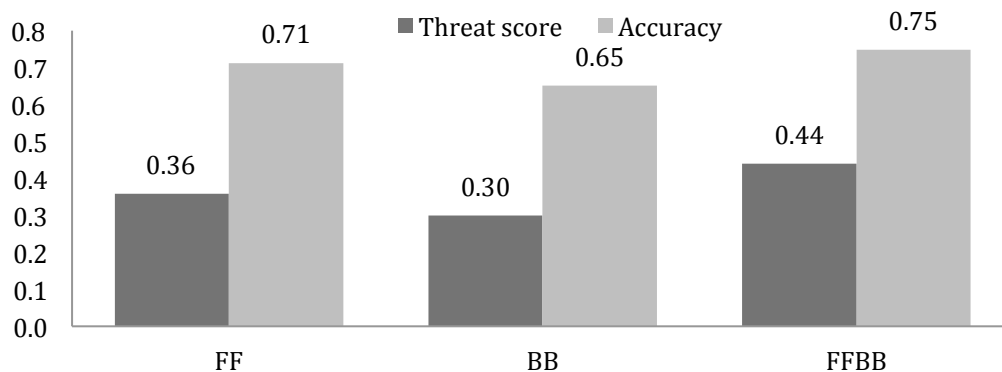
We have estimated *accuracy* based on the Eq. (1):

$$Accuracy = \frac{hits+correct\ negatives}{hits+misses+false\ alarms+correct\ negatives} \quad (1)$$

Accuracy here is also called fraction correct, which is easy to evaluate model prediction. However, it can be misleading for some cases since it is heavily influenced by the most common category, usually "no event" in the case of LVD. Hence, we have provided *threat score* in this study as well. Based on the equation of threat score (or critical success index), we can measure the fraction of observed and/or modeled LVDs that were correctly predicted. Threat score also can be referred as the *accuracy* when correct negatives have been removed from consideration, that is, threat score only concerns modeled LVDs that count.

$$Threat\ Score = \frac{hits}{hits+misses+false\ alarms} \quad (2)$$

The figure below shows the mean value of accuracy and threat score of modeled LVDs among 50 ASEAN cities in three experiments: FF, BB, and FFBB. Since the category of correct negatives is heavily counted in the accuracy, the values are also twice as high as the threat scores. Basically, BB has the lowest threat score while FFBB has the highest score as expected.



The above discussion has been added in Sect. S1 in the supplementary and introduced in the manuscript, Sect. 3.1.

Section 3 should be improved for a better reading, by excluding unnecessary statistical details, and by describing the figures and findings in a more clear and concise way. (abstract and conclusion sections should also be revised).

Based on the reviewer's suggestion, we have removed statistical details (i.e., mostly the standard deviations) in the text (the numbers are still presented in corresponding tables). The structure of the manuscript has been rearranged as well. We have made the manuscript more concise, including the abstract.

Separate section 3.2 into two; first, describe 4 selected cities and your conclusions; then, the entire region.

We have separated Section 3.2 into Sections 3.2 and 3.3 in the revised version. As the reviewer suggested, Section 3.2 now describes results of the 3 selected cities and Section 3.3 discusses those for the entire ASEAN cities.

Section 3.4 is too vague, are you really assessing the impact of aerosols on regional climate? need a better analysis; descriptions are loose; need to cite relevant works throughout the discussion.

We agree with the reviewer that this section diffuses the focus of the paper. We have moved it to supplementary material with a rewriting.

Provide a brief description of machine learning algorithms in the introduction itself (and your motivation for doing this); also, describe it in the method section. Section 4.2 should

be described in an entirely separate section.

Based on the reviewer's suggestion, we have added the motivation of applying machine learning techniques to predict the occurrence of LVDs in the introduction section. We would like to keep the description of each algorithm in the machine learning section to maintain the flow of discussion. Sections 4.1 and 4.2 have been separated into two individual sections in the revised version.

Line 501-503: vague arguments; Line 569-570: describe

Lines 501-503: "Applying inverse modeling, for example, could optimize the emission inventories and hence improve the model performance" has been removed in the revised version.

We have rewrite Line 569-570 to: "Nevertheless, previous works by Reid et al. (2012) and Lee et al. (2017) also suggested the relationships between fire hotspot appearance and certain weather phenomena particularly precipitation. Therefore, we are surprised that precipitation in the fire regions does not appear to be a significant feature for predicting Singapore haze compared with other features in our current analysis."

Reducing the number of figures and tables in the main manuscript (without losing much information) would be helpful; even figure captions are too lengthy.

The reviewer's point has been well received. We have shortened the paper in the revised manuscript. Table 1 has been removed. Table 3, Fig. 7 and Fig. 9 have been moved to the supplementary material. We also have made the captions more concise.

Kurokawa, J., Ohara, T., Morikawa, T., Hanayama, S., Janssens-Maenhout, G., Fukui, T., Kawashima, K., and Akimoto, H.: Emissions of air pollutants and greenhouse gases over Asian regions during 2000–2008: Regional Emission inventory in ASia (REAS) version 2, *Atmos. Chem. Phys.*, 13, 11019-11058, 10.5194/acp-13-11019-2013, 2013.

Lee, H. H., Bar-Or, R. Z., and Wang, C.: Biomass burning aerosols and the low-visibility events in Southeast Asia, *Atmos. Chem. Phys.*, 17, 965-980, 10.5194/acp-17-965-2017, 2017.

Nakanishi, M., and Niino, H.: Development of an Improved Turbulence Closure Model for the Atmospheric Boundary Layer, *Journal of the Meteorological Society of Japan. Ser. II*, 87, 895-912, 10.2151/jmsj.87.895, 2009.

Reid, J. S., Xian, P., Hyer, E. J., Flatau, M. K., Ramirez, E. M., Turk, F. J., Sampson, C. R., Zhang, C., Fukada, E. M., and Maloney, E. D.: Multi-scale meteorological conceptual analysis of observed active fire hotspot activity and smoke optical

depth in the Maritime Continent, Atmos. Chem. Phys., 12, 2117-2147,
10.5194/acp-12-2117-2012, 2012.

Responses to the Comments of the Anonymous Referee #2

We very much appreciate the constructive comments and suggestions from this reviewer. Our point-by-point responses to the reviewer's comments are provided as follows (the reviewer's comments are marked in *Italic font*):

The authors have conducted a very interesting study to investigate the impacts of air pollutants from fire and non-fire emissions on air quality in Southeast Asia. To achieve this goal, they have made use of different sources of data and tools. Overall, I recommend this paper could be published after they have addressed my concerns here.

a) Line 207-211. The model calculates the visibility based on the extinction coefficient of aerosols. The authors neglect the role of relative humidity. Very high relative humidity also leads to low visibility in observations. How will this affect the final result? Can it explain the missing LVD days in the model?

We thank the reviewer for raising this critical point. As indicated in our previous paper (Lee et al., 2017), misty and fog days with high relative humidity have been removed from the observational based LVDs. On the modeling side, the calculation of visibility is indeed based on the extinction coefficient and by also considering the hygroscopic growth of aerosols as a function of relative humidity. We have added necessary statements in the revised manuscript to make this clearer.

It is possible that due to the model resolution, observed relative humidity might not be perfectly reproduced by the model. There are other factors that could limit the performance of the model to reproduce observed LVDs such as missing critical aerosol components in current emission inventories. We have made our best effort to improve the results by, e.g., using aerosol composition measurements to correct modeled aerosol concentrations. We have revised the manuscript accordingly to indicate these potential issues in modeling LVDs.

b) This paper is too long, with 9 tables and 10 figures. The readers don't need to know so many details. So I suggest shortening this paper quite a lot. In my view, these figures and tables can be moved to the supplement. Table 1. You can just mention it in the text. Table 3. You can cite the website where the readers can find the information here. Table 5-8. Try to move some of them to the supplement. Too many details will distract the readers. Figure 6. The readers are lost when they find so much information in this figure. Figure 8-10. Yes, the machine learning techniques used here are very fancy, but they are not the key points of this paper. There is no need to display three figures to illustrate your ML results. Abstract. This is a really long abstract. I suggest shortening it.

The reviewer's point has been well received. We have shortened the paper in the revised manuscript. Table 1 has been removed. Table 3, Fig. 7 and Fig. 9 have been moved to the supplementary material. We would like to keep Fig. 6, Fig. 8 and Fig. 10 in the revised manuscript to support the points that we discuss in the paper. We have shortened the abstract in revised manuscript.

Lee, H. H., Bar-Or, R. Z., and Wang, C.: Biomass burning aerosols and the low-visibility events in Southeast Asia, *Atmos. Chem. Phys.*, 17, 965-980, 10.5194/acp-17-965-2017, 2017.

1
2 **Impacts of air pollutants from fire and non-fire emissions on the regional**
3 **air quality in Southeast Asia**

4 Hsiang-He Lee^{1@}, Oussama Iraqui², Yefu Gu³, Hung-Lam Steve Yim³, Apisada
5 Chulakadabba⁴, Adam Y. M. Tonks⁵, Zhengyu Yang⁶, and Chien Wang^{1,7}

6
7 ¹ Center for Environmental Sensing and Modeling, Singapore-MIT Alliance for Research
8 and Technology, Singapore

9 ²Energy and Environmental Engineering Department, National Institute of Applied Science
10 of Lyon (INSA Lyon), France

11 ³Department of Geography and Resource Management, The Chinese University of Hong
12 Kong, Hong Kong

13 ⁴Department of Civil & Environmental Engineering, Massachusetts Institute of Technology,
14 Cambridge, MA, U.S.A.

15 ⁵Division of Science, Yale-NUS College, Singapore

16 ⁶Department of Mathematics, National University of Singapore, Singapore

17 ⁷Center for Global Change Science, Massachusetts Institute of Technology, Cambridge,
18 MA, U.S.A.
19

20
21 Submitted to

22
23 Atmospheric Chemistry and Physics

24 November 24, 2017

25
26
27 @Corresponding author address: Dr. Hsiang-He Lee, 1 CREATE Way, #09-03 CREATE

28 Tower, Singapore, 138602

29 E-mail: hsiang-he@smart.mit.edu
30

31 **Abstract**

32 Severe haze events in Southeast Asia caused by particulate pollution have become
33 more intense and frequent in recent years, ~~degrading air quality, threatening human~~
34 ~~health, and interrupting economic and societal activities.~~ Widespread biomass burning
35 ~~activities are a major source of severe haze events in Southeast Asia. On the other~~
36 ~~hand, occurrences and~~ particulate pollutants from human activities other than biomass
37 burning ~~also~~ both play ~~an~~ important ~~roles~~ in degrading air quality in Southeast Asia. In
38 this study, numerical simulations have been conducted using the Weather Research and
39 Forecasting (WRF) model coupled with a chemistry component (WRF-Chem) to
40 quantitatively examine the contributions of aerosols emitted from fire (i.e., biomass burning)
41 versus non-fire (including fossil fuel combustion, ~~and road and industrial dust, land use, and~~
42 ~~land change,~~ etc.) sources to the degradation of air quality and visibility over Southeast
43 Asia. These simulations cover a time period from 2002 to 2008 and ~~were~~ ~~are~~ respectively
44 driven by emissions from: (a) fossil fuel burning only, (b) biomass burning only, and (c)
45 both fossil fuel and biomass burning. ~~Across ASEAN 50 cities, these~~ ~~The~~ model results
46 reveal that 39% of observed low visibility days can be explained by either fossil fuel
47 burning or biomass burning emissions alone, a further 20% by fossil fuel burning alone, a
48 further 8% by biomass burning alone, and a further 5% by a combination of fossil fuel
49 burning and biomass burning. ~~The remaining 28% of observed low visibility days remain~~
50 ~~unexplained, likely due to emissions sources that have not been accounted for. Further~~
51 ~~analysis~~ Analysis of 24-hr ~~PM_{2.5}~~ Air Quality Index (AQI) indicates that ~~comparing to the~~
52 ~~simulated result of the case with stand-alone non-fire emissions,~~ the case with coexisting fire
53 and non-fire PM_{2.5} can substantially increase the chance of AQI being in the moderate or
54 unhealthy pollution level from 23% to 34%. The premature mortality among major

55 Southeast Asian cities due to degradation of air quality by particulate pollutants is estimated
56 to increase from ~4110 per year in 2002 to ~6540 per year in 2008. In addition, we
57 demonstrate the importance of certain missing non-fire anthropogenic aerosol sources
58 including anthropogenic fugitive and industrial dusts in causing urban air quality
59 degradation. An ~~exploratory~~ experiment of using machine learning algorithms to
60 ~~forecasting~~forecast the occurrence of haze events in Singapore is also ~~demonstrated~~explored
61 in this study. All these results suggest that besides minimizing biomass burning activities,
62 an effective air pollution mitigation policy for Southeast Asia needs to consider controlling
63 emissions from non-fire anthropogenic sources.

64 **1 Introduction**

65 Severe haze in Southeast Asia has attracted the attention of governments and the
66 general public in ~~the~~ recent years due to its impact on local economy, air quality, and public
67 health (Miettinen et al., 2011; Kunii et al., 2002; Frankenberg et al., 2005; Crippa et al.,
68 2016). Widespread biomass burning activities are one of the major sources of haze events in
69 Southeast Asia. Our previous study demonstrated that biomass burning aerosols contributed
70 to up to 40-60% of haze events in the major cities of Southeast Asia during 2003-2014 (Lee
71 et al., 2017). On the other hand, biomass burning in Southeast Asia could impact climate
72 through emissions of both carbon dioxide (CO₂) (van der Werf et al., 2009) and particulate
73 matter – the latter has a substantial impact specifically on regional climate features including
74 the spatiotemporal distribution of precipitation and energy budgets (Wang, 2004, 2007).

75 Regarding the impact of biomass burning aerosols on public health, a recent study based
76 on the health model in the United States (U.S.) has estimated the number of deaths resulting
77 from black carbon (BC) to be more than 13,500 in 2010 (Li et al., 2016). Considering that

78 both the ambient concentration of particulate matter and overall population in Southeast
79 Asia are higher than those of the U.S., a worse scenario in the region could thus be
80 foreseeable. In fact, a few studies quantifying the consequences of aerosols on human
81 health in Southeast Asia have already suggested taking necessary measures to reduce
82 biomass burning and deforestation in order to prevent related public health issues (Marlier et
83 al., 2013). However, as important as biomass burning pollution may be, it is not the only
84 source of particulate pollution in Southeast Asia. Indeed, aerosols emitted from fossil fuel
85 burning alongside other non-biomass burning human activities, as indicated in our previous
86 study (Lee et al., 2017), also contribute significantly to air quality degradation.

87 Particulate pollutants from human activities other than biomass burning in Southeast
88 Asia include species both locally produced and brought in from neighboring regions by
89 long-range transport. Fossil fuel emissions in Southeast Asia have increased significantly in
90 recent years, especially in areas where energy demands are growing rapidly in response to
91 economic expansion and demographic trends (IEA, 2015). Therefore, advancing our
92 understanding of the respective contributions of aerosols from fire (i.e., biomass burning)
93 versus non-fire (including fossil fuel combustion, road and industrial dust, land use, and land
94 change, etc.) activities to air quality and visibility degradation has become an urgent task for
95 developing effective air pollution mitigation policies in Southeast Asia.

96 In this study, we aim to examine and quantify the impacts of fire and non-fire aerosols
97 on air quality and visibility degradation over Southeast Asia. Three numerical simulations
98 have been conducted using the Weather Research and Forecasting (WRF) model coupled
99 with a chemistry component (WRF-Chem), [which is a sophisticated regional weather-](#)
100 [chemistry model](#), driven respectively by aerosol emissions from: (a) fossil fuel burning only,
101 (b) biomass burning only, and (c) both fossil fuel and biomass burning. By comparing the

102 results of these experiments, we examine the corresponding impacts of fossil fuel and
103 biomass burning emissions, both separately and combined, on the air quality and visibility
104 of the region. [We also use available is-situ measurements to evaluate and correct model](#)
105 [results for providing a better base for further improvement of particularly emissions over the](#)
106 [region. Beyond the traditional process models such as WRF-Chem, we also experiment](#)
107 [using machine learning algorithms to identify suitable conditions for haze based on](#)
108 [historical data and hence to forecast the likelihood of the occurrence of such events in this](#)
109 [study.](#)

110 We firstly describe methodologies adopted in the study, followed by the results and
111 findings from our assessment of the relative contributions of fire and non-fire aerosols in
112 degrading air quality and visibility over Southeast Asia. We then discuss the uncertainty of
113 current emission inventories alongside the results from an exploratory experiment of using
114 machine learning algorithms to [forecastingforecast](#) the occurrence of haze events in several
115 major cities in Southeast Asia. The last section summarizes and concludes our work.

116 **2 Methodology**

117 **2.1 Observational data**

118 **2.1.1 Surface visibility**

119 The observational data of surface visibility from the Global Surface Summary of the
120 Day (GSOD) (Smith et al., 2011) are used in our study to identify the days with low
121 visibility due to particulate pollution, i.e., haze events. The GSOD is derived from the
122 Integrated Surface Hourly (ISH) dataset and archived at the U.S. National Climatic Data
123 Center (NCDC). The daily visibility data are available from 1973 onward.

124 **2.1.2 Particulate matter (PM₁₀)**

125 The surface concentrations of particulate matter with sizes smaller than 10 µm (PM₁₀;
126 measured in µg m⁻³) in Malaysia are derived from the Air Quality Index (AQI; named Air
127 Pollutant Index or API in Malaysia) records obtained from the website of Ministry of
128 Natural Resources and Environment, Department of Environment, Malaysia
129 (http://apims.doe.gov.my/public_v2/home.html). When PM₁₀ is reported as the primary
130 pollutant with a maximum pollutant index, the 24-h~~h~~ PM₁₀ concentrations are calculated
131 from AQI based on the equations in Table S1 (Malaysia, 2000). Data from 51 AQI
132 observation stations are available in Malaysia from October 2005 onward. AQI number is
133 reported twice daily (11 AM and 5 PM local time), and the data reported at 11 AM are used
134 in this study.

135 **2.1.3 Carbon monoxide (CO) and ozone (O₃)**

136 ~~The surface~~Surface mole fractions of CO and O₃ are ~~observed from~~measured by the
137 World Meteorological Organization (WMO) Global Atmosphere Watch (GAW) station in
138 Bukit Kototabang, which is located on the island of Sumatra, Indonesia. Hourly data are
139 archived at the World Data Center for Greenhouse Gases (WDCGG) under the GAW
140 program (<http://ds.data.jma.go.jp/gmd/wdcgg/>).

141 **2.1.4 Crustal matter and residual matter**

142 The Surface PARTiculate mAtter Network (SPARTAN) is a network of ground-based
143 measurements of fine particle concentrations (<http://spartan-network.weebly.com/>)
144 (Snider et al., 2016; Snider et al., 2015). Available data in the SPARTAN network include
145 hourly PM_{2.5} concentrations and certain compositional features (Table S2). Crustal
146 ~~matter~~matters and residual ~~matter~~matters, which are mainly organic components, from

147 filtered PM_{2.5} samples are used in this study to fill the gap in modeled PM_{2.5} created by the
148 missing anthropogenic ~~dust~~aerosol in emission inventory (Philip et al., 2017). The four
149 operational SPARTAN sites in Southeast Asia are Bandung (Indonesia), Hanoi (Vietnam),
150 Manila (~~Philippine~~Philippines), and Singapore (Singapore). The chemical components of
151 PM_{2.5} in each city are presented in Fig. S1.

152 **2.2 The model**

153 WRF-Chem version 3.6.1 is used in this study to simulate trace gases and particulates
154 interactively with the meteorological fields using several treatments for photochemistry and
155 aerosols (Grell et al., 2005). We selected the Regional Acid Deposition Model, version 2
156 (RADM2) photochemical mechanism (Stockwell et al., 1997) coupled with the Modal
157 Aerosol Dynamics Model for Europe (MADE), which includes the Secondary Organic
158 Aerosol Model (SORGAM) (Ackermann et al., 1998; Schell et al., 2001), to simulate
159 anthropogenic aerosols evolution in Southeast Asia. MADE/SORGAM uses a modal
160 approach (including Aiken, accumulation, and coarse modes) to represent the aerosol size
161 distribution, and predicts mass and number for each aerosol mode. The numerical
162 simulations are employed within a model domain with a horizontal resolution of 36 km,
163 including 432 × 148 horizontal grid points (Fig. 1), and 31 vertically staggered layers based
164 on a terrain-following pressure coordinate system. ~~The domain covers an area from the~~
165 ~~Indian Ocean to~~The Mellor-Yamada-Nakanishi-Niino level 2.5 (MYNN) (Nakanishi and
166 Niino, 2009) is chosen as the planetary boundary scheme in this study. By using a vertical
167 coordinate that is stretched to have higher resolutions inside the planetary boundary layer,
168 the model has about 4-5 vertical layers inside the planetary boundary layer with a vertical
169 resolution of ~30 m near the surface. The domain covers an area from the Indian Ocean to
170 the Western Pacific Ocean in order to capture the Madden-Julian Oscillation (MJO) pattern.

171 The time step is 180 seconds for advection and physics calculation. The physics schemes
172 ~~included in the simulations are listed in Table 1.~~ in the simulations include Morrison (2
173 moments) microphysics scheme (Morrison et al., 2009), RRTMG longwave and shortwave
174 radiation schemes (Mlawer et al., 1997; Iacono et al., 2008), Unified Noah land-surface
175 scheme (Tewari et al., 2004), and Grell-Freitas ensemble cumulus scheme (Grell and
176 Freitas, 2014). The initial and boundary meteorological conditions are taken from the U.S.
177 National Center for Environment Prediction FiNaL (NCEP-FNL) reanalysis data (National
178 Centers for Environmental Prediction, 2000), which has a spatial resolution of 1 degree and
179 a temporal resolution of 6 hours. Sea surface temperatures are updated every 6 hours in
180 NCEP-FNL. All simulations used a four-dimensional data assimilation (FDDA) method to
181 nudge NCEP-FNL temperature, water vapor, and zonal as well as meridional wind speeds
182 above the planetary boundary layer ~~(PBL).~~

183 **2.3 Emission inventories**

184 The Regional Emission inventory in ASia (REAS) version 2.1 (Kurokawa et al., 2013)
185 is a regional emission inventory for Asia, including monthly emissions of most major air
186 pollutants, e.g., black carbon (BC), organic carbon (OC), sulfur dioxide (SO₂), nitrogen
187 dioxide (NO₂), and greenhouse gases between 2000 and 2008. The spatial resolution of
188 REAS is 0.25 × 0.25 degrees, covering East, Southeast, South, and Central Asia and the
189 Asian part of Russia (Russian Far East, Eastern and Western Siberia, and the Ural). The
190 area coverage of REAS is from 60°E to 160°E in longitude and from 10°S to 50°N in
191 latitude, which is smaller than our domain configuration. For this reason, we use the
192 Emissions Database for Global Atmospheric Research (EDGAR) version 3.2 (the year 2000
193 emission) (Olivier et al., 2005) and version 4.2 (the year 2005 emission)
194 (<http://edgar.jrc.ec.europa.eu>) to complement the emissions over areas outside REAS

195 coverage. The emission coverage of REAS and EDGAR in our simulated domain is
196 presented in Fig. 1. [We have compared the modeled results using REAS versus EDGAR](#)
197 [emission inventories in a set of one-year paired simulations: the differences between these](#)
198 [two model runs are rather limited regarding aerosol-related variables \(Table S3\). After](#)
199 [considering high spatiotemporal resolution of REAS emission inventory and the comparison](#)
200 [results, we decided to use REAS in this study. In addition, a detailed comparison of REAS](#)
201 [with other emission inventories in Southeast Asia was also presented by Kurokawa et al.](#)
202 [\(2013\).](#)

203 The Fire INventory from U.S. National Center for Atmospheric Research (NCAR)
204 version 1.5 (FINNv1.5) (Wiedinmyer et al., 2011) is also used in the study to provide fire-
205 based emissions. FINNv1.5 classifies burnings of ~~extra-tropical~~[extratropical](#) forest, tropical
206 forest (including peatland), savanna, and grassland. The daily data are available from 2002
207 to 2014 with a 1 km spatiotemporal resolution. FINNv1.5 emission inventory also includes
208 the major chemical species (e.g., BC, OC, SO₂, CO, and NO₂) from biomass burning. A
209 modified plume rise algorithm in WRF-Chem, specifically for tropical peat fire, is described
210 in Lee et al. (2017).

211 Compared ~~to~~[with](#) fossil fuel emissions, biomass burning emissions vary in space and
212 time (Fig. [S1-S2](#)). However, regarding long-term impact, both emissions are important to
213 regional air quality in Southeast Asia (Table [21](#)). BC from biomass burning emissions, for
214 example, has significant inter-annual and inter-seasonal variabilities due to the Southeast
215 Asia monsoon and the El Niño-Southern Oscillation (ENSO) (Lee et al., 2017; Reid et al.,
216 2012), but total BC emissions are equally contributed by fossil fuel and biomass burning
217 sources (Table [21](#)).

218 2.4 Numerical experiment design

219 Three numerical simulations are proposed to investigate the impacts of fire and non-fire
220 aerosols on regional air quality and visibility in Southeast Asia. Among these three runs, the
221 fossil fuel emissions only (FF) simulation and the biomass burning emissions only (BB)
222 simulation are designed to ~~aeess~~assess the impact of stand-alone non-fire and fire aerosols,
223 respectively. The simulation combining both fossil fuel and biomass burning emissions
224 (FFBB) is to demonstrate the impacts of both types of aerosols; it is also closer to real world
225 case than the two other runs. Based on available years of emission inventories, each of these
226 runs lasts 7 years (i.e., from 2002 to 2008).

227 2.5 Deriving “Low Visibility Day” (LVD) caused by particulate pollution

228 According to Visscher (2013), a visibility reading lower than 10 km is considered a
229 moderate to heavy air pollution event by particulate matter. As in Lee et al. (2017), we
230 define a “low visibility day (LVD)” when the daily-mean surface visibility is lower or equal
231 to 10 km, ~~not including misty and fog days~~. The modeled visibility is calculated based on
232 the extinction coefficient of the externally mixed aerosols, including BC, OC, sulfate (SO_4^{2-})
233 and nitrate (NO_3^-), as a function of particle size, by assuming a log-normal size distribution
234 of Aitken and accumulation modes. Note that all these calculations are computed for the
235 wavelength of 550 nm. To make the calculated visibility ~~of the~~based on modeled aerosols
236 better match the reality, we ~~have also considered~~consider the hygroscopic growth of OC,
237 sulfate, and nitrate in the calculation based on the modeled relative humidity (Kiehl et al.,
238 2000; Lee et al., 2017).

239 Our focus in this study is to first identify LVDs and then to determine whether fire or
240 non-fire aerosols alone, or in combination, could cause the occurrence of these LVDs. As a

241 reference, the observed low visibility days ~~were~~are identified and the annual frequency in
242 every year for a given city ~~were~~are also derived by using the GSOD visibility data. Then,
243 the modeled low visibility days ~~were~~are derived following the same procedure. Using these
244 results and based on the logical chart in Fig. 2, the major particulate source (FF, BB or
245 FFBB) that caused the occurrence of observed LVDs ~~were~~are determined. Here, Type 1
246 LVD represents the cases where either fire or non-fire aerosols alone can cause the observed
247 LVD to occur. Type 2 means that non-fire aerosols are the major contributor to the
248 observed LVD. Type 3 ~~is the same as Type 2 but caused by means that~~ fire aerosols are the
249 major contributor to the observed LVD. Type 4 represents the cases where the observed
250 LVD is induced by coexisting fire and non-fire aerosols. The observed LVDs that the model
251 cannot capture are classified as Type 5.

252 2.6 Air Quality Index (AQI)

253 The Air Quality Index is established mainly for the purpose to provide easily
254 understandable information about air pollution to the public. The original derivation of AQI
255 in the U.S. is based on six pollutants: particulate matter (PM₁₀), fine particulate matter
256 (PM_{2.5}), sulfur dioxide (SO₂), carbon monoxide (CO), ozone (O₃), and nitrogen dioxide
257 (NO₂). Each pollutant is scored on a scale extending from 0 through 500 based on the
258 corresponding breakpoints, and then the highest AQI value is reported to the public. In this
259 study, we focus on the AQI derived from modeled 24-hr PM_{2.5} and 9-hr O₃. Note that the
260 original AQI is derived by using 8-hr O₃. Due to the 3-hr output interval of simulated O₃,
261 we use the 9-hr O₃ level instead in this study. An index I_p for pollutant p is calculated by
262 using a segmented linear function that relates pollutant concentration, C_p :

$$263 \quad I_p = \frac{I_{Hi} - I_{Lo}}{B_{Hi} - B_{Lo}} (C_p - B_{Lo}) + I_{Lo}, \quad (1)$$

264 where B_{Hi} is the upper breakpoint of C_p satset category and B_{Lo} is the bottom breakpoint of
265 C_p sat category in Table 3S4. I_{Hi} and I_{Lo} are the AQI values corresponding to B_{Hi} and B_{Lo} ,
266 respectively. For example, when the ~~24-h~~24-h PM_{2.5} concentration is 20 $\mu\text{g m}^{-3}$, B_{Hi} , B_{Lo} ,
267 I_{Hi} , and I_{Lo} are 12,1, 35.4, 51 and 100, respectively. Then, we selected 24-h~~h~~ PM_{2.5} and the
268 maximum 9-h~~h~~ O₃ AQI value in one day to represent daily AQI for PM_{2.5} ($\text{AQI}_{(\text{PM}_{2.5})}$) and
269 O₃ ($\text{AQI}_{(\text{O}_3)}$), respectively.

270 2.7 Health Impact Assessment (HIA)

271 Previous observations have revealed significantly higher PM_{2.5} concentrations in the
272 cities of Southeast Asia than those in America and Europe (WHO, 2016), implying that the
273 concentration-response functions (CRFs) derived from the latter places may not be directly
274 applicable to Southeast Asia. In this study, we ~~adapted~~adapt CRFs in Gu and Yim (2016) to
275 estimate the annual number of premature mortalities due to ambient PM_{2.5} concentration in
276 the corresponding region. The relative risk (RR) of four causes of death, including chronic
277 obstructive pulmonary disease, ischemic heart disease, lung cancer, and stroke, when
278 compared with annual incident rate, have been assessed separately. Such risks ~~were~~are
279 described by a log-linear relationship with the corresponding PM_{2.5} concentration level
280 (Burnett et al., 2014). The basic form of RR formulas is provided as follows:

$$281 \quad RR = 1 + \alpha \cdot \left\{ 1 - \exp \left[-\beta (X_j - X_0)^\delta \right] \right\}, \quad (2)$$

282 where X_j and X_0 are the particulate pollutant concentrations ($\mu\text{g m}^{-3}$) in the target cities and
283 the threshold value below which no additional risk is assumed to exist, respectively. Here
284 we present the uncertainty range of threshold value between 5.8 $\mu\text{g m}^{-3}$ and 8.8 $\mu\text{g m}^{-3}$ in a
285 triangular distribution, as suggested by the GBD 2010 project (Lim et al., 2013).

286 Epidemiological results are not always available in Southeast Asia. To capture both
287 climbing and flattening out phases of CRFs curves suitable for Southeast Asia region, we
288 ~~fitted~~fit parameters α , β , and δ in CRFs by the epidemiological samples in the East Asian
289 cities based on Gu and Yim (2016) for China, where PM_{2.5} concentration has a comparable
290 level to that in Southeast Asia.

291 The form of integrated CRF is calculated by the following formula:

$$292 \quad E = \sum_j (RR_j - 1) / RR_j \cdot P_j \cdot f_j, \quad (3)$$

293 where P refers to the population in the researched cities from 2002 to 2008, retrieved from
294 statistics in their respective countries (DSM, 2010; NSCB, 2009; NSOT, 2010; CSOM,
295 2010; GSOV, 2009; DSS, 2008, 2016; NISC, 2013; BPS, 2009). f denotes the baseline
296 incident rate above 30 years of age (WHO, 2017).

297 **3 Results**

298 **3.1 Model evaluation**

299 Multiple ground-based observations are used in this study to evaluate the model's
300 performance particularly in simulating aerosol and major gaseous chemical species such as
301 ozone and carbon monoxide. PM_{2.5} observations in Southeast Asia are very limited,
302 ~~especially for the modeling period of this study.~~ Even in Singapore, observed PM_{2.5} data
303 are only available after 2014 for the general public and research community to access.
304 Therefore, PM₁₀ concentrations derived from AQI in Kuala Lumpur (Malaysia) are used to
305 present the variation of particulate matter during haze and non-haze seasons. Comparing
306 with the observations, the model accurately predicted PM₁₀ concentration, especially during
307 haze seasons (July to October) (Fig. 3a); however, it produced a systematic negative bias

308 of 20 $\mu\text{g m}^{-3}$ in background PM_{10} concentration during non-haze periods. This discrepancy
309 between modeled and observed background PM_{10} concentration could come from either the
310 relatively coarse resolution of the model or the underestimation of [primary aerosol](#)~~/or/~~
311 aerosol precursor emissions, or both. Philip et al. (2017) indicated that most global emission
312 inventories do not include anthropogenic fugitive, combustion, and industrial dust (AFCID)
313 from urban sources, typically including fly ash from coal combustion and industrial
314 processes (e.g. iron and steel production, cement production), resuspension from paved and
315 unpaved roads, mining, quarrying, and agricultural operations, and road-residential-
316 commercial construction. In their study, they estimated a ~~2—~~ 2– 16 $\mu\text{g m}^{-3}$ increase in fine
317 particulate matter ($\text{PM}_{2.5}$) concentration across East and South Asia simply by including
318 AFCID emission. [We also find that the major component of \$\text{PM}_{2.5}\$ particles from the](#)
319 [filtered samples of SPARAN observational network is residual materials, which are mainly](#)
320 [organic matters \(Snider et al., 2016\) \(Fig. S1\). All of these analyses show the incompleteness](#)
321 [in the current emission inventories.](#) In addition to PM_{10} data, we have also used observed
322 [surface](#) visibility to evaluate model performance. As mentioned in Sect. 2.5, the modeled
323 visibility values are derived from the extinction coefficient of the externally mixed aerosols
324 and simulated fine particulate concentrations. As shown in Fig. 4, the model correctly
325 predicted about 40% observed low-visibility events during the fire seasons, while 60% miss-
326 captured low-visibility events are mainly due to the missing AFCID. The details of this are
327 discussed in Sect. 4.4. [Additional uncertainty analysis of modeled LVDs by using a method](#)
328 [for dichotomous \(yes or no LVDs\) cases is presented in Sect. S1 of the supplementary](#)
329 [material.](#) On the other hand, the model has overestimated the visibility range for many cases
330 with observed visibility lower than 7 km. Such ~~an underestimate~~ [result](#) is likely due to the
331 36-km model resolution used in the study, which could be too coarse to resolve the typical

332 size of air plumes containing high concentration of fine particulate matters. [The detailed](#)
333 [discussion of potential uncertainty factors of modeled visibility, including meteorological](#)
334 [datasets, fire emission inventories, and the model resolution can be found in Lee et al.](#)
335 [\(2017\).](#)

336 The observed CO and O₃ levels ~~is~~from the only WMO GAW station in the region,
337 Bukit Kototabang, Indonesia (West Sumatra) are used to evaluate the model performance in
338 simulating gas phase chemistry. Fossil fuel and biomass combustions and biogenic
339 emissions are among the major sources of CO in the region, while O₃ production is mainly
340 ~~resulted~~from photochemical reactions of precursors such as nitrogen oxides, volatile
341 organic compounds, and CO, largely from anthropogenic emissions. Due to ~~is~~the
342 geographic location, the primary source of CO in Bukit Kototabang is from biomass burning,
343 ~~and~~hence high CO levels ~~hence~~ occur during fire seasons (Fig. 3b). The model accurately
344 captured observed CO levels during the simulation. ~~Model simulated evolution of volume~~
345 ~~mixing ratio of O₃ also very well matches observations, though with a positive bias of about~~
346 ~~20 ppbv on average (34.8±10.1 versus 13.4±6.1 ppbv) (Fig. 3e).~~ [Model simulated evolution](#)
347 [of volume mixing ratio of O₃ also matches observations very well, though with a positive](#)
348 [bias of about 20 ppbv on average \(34.8 versus 13.4 ppbv\) \(Fig. 3c\).](#) We notice that NO_x
349 [emission is higher in REAS emission inventory comparing with other emission inventories](#)
350 [and studies \(Kurokawa et al., 2013\). The boundary condition of WRF-Chem also sets the](#)
351 [background surface ozone quite high \(30 ppbv\). Both could lead to the overestimated](#)
352 [background ozone in the model.](#)

353 **3.2 Fire- and non-fire-caused LVDs in ~~four~~three selected cities ~~and over the~~**
354 **~~whole Southeast Asia~~**

355 ~~By comparing the annual mean $PM_{2.5}$ concentration in 50 Association of Southeast~~
356 ~~Asian Nations (ASEAN) cities between three simulations, we identify that there are 13~~
357 ~~ASEAN cities receiving more than 70% $PM_{2.5}$ concentration from non-fire sources, while~~
358 ~~there are 10 ASEAN cities where fire aerosols are the major (more than 70%) component of~~
359 ~~$PM_{2.5}$ (Fig. 5). Note that although fire aerosols are the major component of annual mean~~
360 ~~$PM_{2.5}$ concentration in these 10 ASEAN cities, the influence period of fire aerosols normally~~
361 ~~is only about 3 to 5 months. The rest of the ASEAN cities are essentially influenced by~~
362 ~~coexisting fire and non-fire aerosols. Note that the sum of $PM_{2.5}$ concentrations in FF and~~
363 ~~DB is not necessarily equal to the $PM_{2.5}$ concentration in FFDB in any given city due to non-~~
364 ~~linearity in modeled aerosol processes.~~

365 Based on the logical chart shown in Fig. 2, we can use the modeled results to classify
366 observed LVDs into 5 types of events with different main aerosol sources. In Bangkok,
367 there are about 165 ± 14 LVDs (~~$45 \pm 4\%$~~) per year during 2002-2008 based on observations.
368 Modeled results suggest that about 60% of these LVDs can be brought by either fire or non-
369 fire aerosols (the sum of Type 1, Type 2, and Type 3 in Fig. 2; see Table 42). Generally
370 speaking, fire and non-fire aerosols contribute equally towards the haze events occurring in
371 Bangkok. A more interesting finding is that $11 \pm 4\%$ of LVDs need a combination of both
372 fire and non-fire aerosols to occur (Type 4). This highlights the importance of fire aerosols
373 in worsening air quality of otherwise moderate haze conditions under the existing suspended
374 non-fire aerosols. Overall, the model missed about $29 \pm 5\%$ of LVDs of Bangkok during the
375 simulation period.

376 Haze occurs slightly less frequently in Kuala Lumpur than Bangkok. There are about
377 104 ± 51 LVDs ($29 \pm 14\%$) per year in Kuala Lumpur during 2002-2008. Thirty-six percent of
378 these LVDs are caused by either fire or non-fire aerosols; while $15 \pm 6\%$ of the LVDs need a
379 combination of both aerosol sources to form haze (Table 42). Our study shows that non-fire
380 aerosols are capable of causing of 28% of LVDs occurring in Kuala Lumpur, even in the
381 absence of fire aerosols. Once we include the impact of fire aerosols, the model can capture
382 an additional 23% of LVDs, of which most are Type 4 case. Overall, fire and non-fire
383 aerosols make similar contributions to observed LVDs in Kuala Lumpur.

384 In Singapore, there are about 50 ± 14 LVDs ($14 \pm 4\%$) per year during 2002-2008. The
385 contribution of non-fire aerosols to LVDs is about 8%. Compared ~~to~~with the additional
386 25% of LVDs owing to fire aerosols, the contribution of non-fire aerosols to LVDs is small
387 in Singapore. However, the model failed to capture a high percentage of LVD cases in both
388 Kuala Lumpur ($49 \pm 26\%$) and Singapore ($67 \pm 21\%$) (Type 5; see Table 42). As discussed in
389 Sect. 3.1, missing AFCID in the emission inventory could explain why the model failed to
390 capture the LVDs in these two sites. Further discussion is presented in Sect. 4.1.

391 **3.3 Fire- and non-fire-caused LVDs over the whole Southeast Asia**

392 By comparing the annual mean $PM_{2.5}$ concentration in 50 Association of Southeast
393 Asian Nations (ASEAN) cities between three simulations, we identify that there are 13
394 ASEAN cities receiving more than 70% $PM_{2.5}$ concentration from non-fire sources, while
395 other 10 ASEAN cities where fire aerosols are the major (more than 70%) component of
396 $PM_{2.5}$ (Fig. 5). Note that although fire aerosols are the major component of annual mean
397 $PM_{2.5}$ concentration in these latter 10 ASEAN cities, the influence period of fire aerosols
398 normally is only about 3 to 5 months. The rest of the ASEAN cities are essentially
399 influenced by coexisting fire and non-fire aerosols. Note that the sum of $PM_{2.5}$

400 concentrations in FF and BB is not necessarily equal to the PM_{2.5} concentration in FFBB in
401 any given city due to non-linearity in modeled aerosol processes.

402 The annual mean LVDs among 50 ASEAN cities is 192±8 days (~~53±2%~~) during 2002-
403 2008. Applying the logical chart described in Fig. 2 to analyze cases of each of these
404 ASEAN cities, we find that by considering aerosols emitted from non-fire emissions alone,
405 about 59% of observed LVDs can be explained, whereas considering fire aerosols adds an
406 additional 13% of LVDs. Conversely, by considering aerosols emitted from fire ~~alongalone,~~
407 about 47% of observed LVDs can be explained, whereas adding non-fire aerosols adds an
408 additional 25% of LVDs. ~~Two-eight-percent~~ About 28% of observed LVDs remains
409 unexplained. In general, non-fire aerosols appear to be the major contributor to LVDs in
410 these cities.

411 **3-3.4 Impacts of ozone and PM_{2.5} on air quality and human health**

412 Similar to PM_{2.5}, O₃ also brings public ~~concerns~~-health besides air quality issues (Chen
413 et al., 2007). Previously, in Sect. 3.1, we have discussed that the model systematically
414 overestimated O₃ volume mixing ratio by 20 ppbv comparing ~~to~~with observations.
415 Overestimated ~~9-hh~~ O₃ ~~will~~could lead to a mistakenly derived high AQI_(O₃). Nevertheless,
416 the relative differences of AQI_(O₃) between various model simulations can still provide
417 useful information of the relative contributions of fire and non-fire emissions, either alone or
418 in combination, on air quality and potentially human health.

419 We find that modeled ~~9-hh~~ O₃ in Bangkok from non-fire emissions (FF) alone
420 triggered 19% of daily AQI_(O₃) to reach moderate and unhealthy pollution level during 2002-
421 2008, while fire emissions (BB) alone can only trigger 3% of such ~~situations~~situations (Table
422 53). In comparison, combining fire and non-fire emissions as derived from the simulation of
423 FFBB can cause 33% of daily AQI_(O₃) to reach moderate and unhealthy pollution

424 ~~level~~levels. In Kuala Lumpur and Singapore, O₃ is not the major source for air quality
425 degradation, where fire or non-fire emissions alone can seldom cause O₃ levels to reach
426 even moderate pollution levels. For example, in the FF simulation, only 5% of daily AQI_(O₃)
427 readings in Kuala Lumpur and 1% in Singapore reached moderate pollution levels. Again,
428 the majority of the high AQI_(O₃) cases result from combining fire and non-fire emissions
429 (FFBB) (Table 53). Overall, non-fire emissions alone only cause 6% of daily AQI_(O₃) to
430 reach moderate pollution levels in 50 ASEAN cities, whereas about 12% of moderate and
431 unhealthy pollution cases resulted from the combined effect of fire and non-fire emissions.

432 We find that in Southeast Asia, PM_{2.5} actually plays a more important role than O₃ in
433 causing high AQI cases. In Bangkok, PM_{2.5} resulted in 37% and 33% high daily AQI_(PM_{2.5})
434 cases ~~in~~ FF and BB simulation, respectively (Table 64). Among these, three times more
435 cases with daily AQI_(PM_{2.5}) reaching unhealthy levels can be attributed to PM_{2.5} from BB
436 than those from FF (Table 64). However, the unhealthy levels caused by fire aerosols alone
437 still occur relatively infrequently in Bangkok, Kuala Lumpur, and Singapore. In Bangkok, a
438 city with an 8 million population, persistent aerosol emissions from non-fire sources, aided
439 by seasonal fire aerosols, cause almost two-thirds of daily air quality readings ~~to reach that~~
440 ~~reached~~ moderate or unhealthy pollution levels. Kuala Lumpur and Singapore also have
441 48% and 22% bad air quality days during 2002-2008, respectively (Table 64). Examining
442 ~~24-hr~~ PM_{2.5} AQI_(PM_{2.5}) among 50 ASEAN cities shows that non-fire aerosols alone
443 contribute to moderate to unhealthy pollution levels 2.6 times more often than fire aerosols
444 alone (23% versus 9%). Compared to the modeled results in FF, PM_{2.5} in FFBB increases
445 10% more bad air quality to moderate and unhealthy pollution level (Table 64). This result
446 is consistent with the findings in Sect. 3.23.

447 We have examined the health impacts due to PM_{2.5} in 50 ASEAN cities using the
448 method described in Sect. 2.7 and the results show that the top three cities for premature
449 mortality caused by particulate pollution are Jakarta (Indonesia), Bangkok (Thailand), and
450 Hanoi (Vietnam) with 910, ~~4076~~1080, and ~~6246~~20 premature mortalities per year,
451 respectively (Fig. 6). The premature mortality in Jakarta is mainly due to exposure to PM_{2.5}
452 particles emitted from non-fire emissions (95%), the same situation as in Hanoi (80%).
453 However, in Bangkok, the health impact due to fire and non-fire aerosols are equally critical
454 (Figs. ~~S2S3~~ and ~~S3S4~~). In general, owing to the increasing trend of non-fire emissions
455 during the analysis period, the premature mortalities due to PM_{2.5} emitted from non-fire
456 sources have increased with time in most ASEAN cities (Fig. ~~S2S3~~). Besides this, higher
457 fire aerosols levels in Sumatra and Borneo in 2002, 2004 and 2006 also ~~increased~~increase
458 the number of premature mortalities in cities such as Kuching, which ~~were~~are exposed to
459 particulate matters from these burning events (Figs. 6 and ~~S3~~S4).

460 ~~3.4~~ The Additional discussion of the impact of fire and non-fire aerosols on 461 regional climate

462 ~~Besides influencing surface and air temperature through scattering and absorbing solar~~
463 ~~radiation, aerosols can also alter the spatiotemporal patterns of precipitation via aerosol~~
464 ~~direct and indirect effects (Wang, 2015). Over the modeled domain, rainfall (is presented in~~
465 ~~quantity) mainly comes from convective clouds. When the model is configured with a~~
466 ~~relatively coarse resolution as adopted in our study, however, the convective precipitation~~
467 ~~process is calculated through the cumulus parameterization of the model, which follows a~~
468 ~~mass flux approach to diagnose rainfall and does not interact with aerosols. Despite of this~~
469 ~~drawback, aerosols can still influence the radiation budget through their direct effect. The~~

Formatted: Font color: Accent 1

470 thermodynamic consequences of this effect can further influence the cloud formation. On
471 the other hand, the model does contain aerosol-cloud microphysical interaction for
472 stratiform clouds; therefore, aerosols can influence these clouds through the so-called
473 indirect effects by providing cloud condensation nuclei for cloud droplets to form. Hence,
474 cumulus rainfall can be still affected indirectly through dynamical and thermodynamic
475 processes initiated by either aerosol direct effects, indirect effects in stratiform clouds, or
476 both. Sect. S2 of the supplementary.

477 By comparing the precipitation in FF and FFBB, we have examined the impact of the
478 extra forcing from fire aerosols on precipitation in the modeled Southeast Asia domain
479 (10°S – 20°N in latitude, 90°E – 150°E in longitude). Non-fire aerosols provide a baseline
480 pattern because of the persistency of fossil fuel emissions, while biomass burning emissions
481 load additional aerosols in the air to alter total aerosol radiative forcing, which then would
482 change precipitation. Through aerosol direct and indirect effects, the difference of monthly
483 regional mean downward shortwave radiation at surface is $8.8 \pm 4.3 \text{ W m}^{-2}$ ($232.6 \pm 19.0 \text{ W m}^{-2}$
484 in FF versus $223.8 \pm 20.1 \text{ W m}^{-2}$ in FFBB; Fig. S4). The data are calculated over land only.
485 Owing to the reduction of surface incoming solar radiation by fire aerosols, surface skin
486 temperature is $0.2 \pm 0.2 \text{ K}$ lower in FFBB than in FF (Fig. S5). Lower surface temperature
487 brought by fire aerosols would suppress convection (Berg et al., 2013). As a result, the
488 model produced a lower monthly regional mean precipitation in FFBB than in FF by 0.2 ± 0.4
489 mm day^{-1} over land ($11.15 \pm 4.27 \text{ mm day}^{-1}$ versus $11.35 \pm 4.42 \text{ mm day}^{-1}$; Fig. 7), with the
490 most significant rainfall changes occurring in the fire emission regions of Sumatra and
491 Borneo. We also find higher cloud water mass in FFBB, which has stronger radiative
492 forcing than aerosols. Nevertheless, further study using a cloud-resolving resolution is
493 necessary.

4 Discussion

4.1 Uncertainty of emission inventory

4 Impact of missing components in the emission inventories on modeled results

In this study, we have noticed ~~that~~ the simulated PM_{2.5} concentrations in Singapore are often lower than the observations of the National Environment Agency of Singapore (<https://data.gov.sg/dataset/air-pollutant-particulate-matter-pm2-5>) (6.1 µg m⁻³ versus 20.3 µg m⁻³ in annual mean during 2002-2008). Owing to the lower simulated PM_{2.5} concentration in Singapore, the model could not capture many observed LVDs (Table 4.2) and consequently underestimated AQI levels resulting from PM_{2.5}. As mentioned before, Philip et al. (2017) have pointed out that global atmospheric models can produce a 2–16 µg m⁻³ underestimation in fine particulate mass concentration across East and South Asia ~~due to a lack of inclusion of anthropogenic fugitive, combustion and industrial dust emissions in the emission inventories.~~ ~~Most and most~~ current global emission inventories indeed either do not include anthropogenic fugitive and industrial dusts, or substantially underestimate the quantities of these emissions (Klimont et al., 2016; Janssens-Maenhout et al., 2015). The fugitive dust sources, such as road and construction dust, in most major cities in Southeast Asia are apparently not well represented in the emission inventory used in our study. To correct these systematic underestimates, we have used crustal matter and residual matter from ~~filtered~~ SPARTAN PM_{2.5} measurements as the reference to fill in the modeled PM_{2.5} for the missing anthropogenic ~~dust component~~ aerosol components. Excluding the high concentration samples during the fire haze events, the mean concentration of crustal matter and residual matter is 25.8 µg m⁻³ in Hanoi, 10.4 µg m⁻³ in

517 Singapore, $18.1 \mu\text{g m}^{-3}$ in Bandung, and $9.2 \mu\text{g m}^{-3}$ in Manila. We then added these values
518 as ~~the additional~~ anthropogenic ~~dust aerosol~~ components in modeled aerosol abundance to
519 recalculate modeled visibility and $\text{AQI}_{(\text{PM}_{2.5})}$. Table 75 shows the calculated percentage of
520 LVDs caused by various aerosol types in Fig. 2 before and after the above correction.

521 Adding the ~~missing~~ anthropogenic ~~dust aerosol~~ component based on in-situ
522 measurement in the modeled results can reproduce 98% of observed LVDs in Hanoi (an
523 increase from 79%). Because the missing anthropogenic ~~dust aerosols~~ are included in non-
524 fire aerosols, LVDs in Type 1 and Type 2 are heavily weighted in the new result. The
525 results also show the LVDs in Hanoi are mainly caused by non-fire aerosols and the
526 contribution of fire aerosols is relatively small. Adding ~~the missing~~ anthropogenic
527 ~~dust aerosol~~ components also reduced the number of missing LVDs events from 67% to 20%
528 in Singapore. Differing from Hanoi, not only Type 2 LVDs but also Type 4 LVDs increased
529 after introducing the missing anthropogenic ~~dust aerosols~~ in Singapore, implying that the
530 fire and non-fire aerosols are equally important in causing LVDs there. After applying the
531 correction, non-fire aerosols alone can explain 30% LVDs while coexisting fire and non-fire
532 aerosols can explain 40% LVDs in Singapore (Table 75). Note that the mode of the
533 distribution of observed visibility in Singapore is around 11 km. Therefore, when fire
534 occurs in the surrounding countries, even a moderate addition to the aerosol abundance from
535 fire can worsen visibility to reach a low visibility condition (visibility < 10 km). Because of
536 the poor data quality of observed visibility in Bandung (only less than 10% observations are
537 available), introducing the missing anthropogenic ~~dust aerosol components~~ did not help to
538 characterize the major aerosol contribution. In Manila, the number of missed LVDs in the
539 model reduced 35% while Type 2 and Type 4 LVDs increased 26% and 9%, respectively,
540 after introducing the missing anthropogenic ~~dust aerosol components~~. Nevertheless, even

541 after adding [the missing](#) anthropogenic ~~dusts in aerosols to the~~ non-fire aerosol category, the
542 model still missed 57% of LVDs in Manila. This is mainly because the model did not
543 capture many fire events in that area, likely due to underestimation of fire emissions in the
544 emission inventory.

545 Besides LVDs, the missing anthropogenic ~~dusts aerosols~~ also substantially affect the
546 ~~modelled~~[modeled](#) AQI_(PM2.5). Table [86](#) shows the frequency of various AQI_(PM2.5) levels
547 calculated respectively with and without the missing anthropogenic ~~dusts aerosol~~
548 [components](#) in Hanoi, Singapore, Bandung, and Manila. After considering the missing
549 anthropogenic ~~dusts aerosol components~~, modeled air pollution levels in Hanoi and Bandung
550 persistently reach the moderate or unhealthy pollution levels. In Singapore, modeled
551 frequency of moderate and unhealthy cases also increase from 22% to 66%, and in Manila
552 from 8% to 36%. Furthermore, the number of premature mortalities in Singapore and
553 Manila increases significantly from 0 to 230 and ~~128~~[130](#), respectively (Table [97](#)). These
554 results indicate the importance for models to include anthropogenic fugitive and industrial
555 ~~dust~~[dusts](#) in order to capture low visibility events in the region.

556 ~~Model resolution, the accuracy of both fire and non fire emissions, and other potential~~
557 ~~aerosol sources all could cause the model bias in capturing observed LVDs and thus~~
558 ~~underestimate the air pollution levels and associated health impacts. Among those possible~~
559 ~~factors, the fire and non fire emission inventories are the most critical. Applying inverse~~
560 ~~modeling, for example, could optimize the emission inventories and hence improve the~~
561 ~~model performance.~~

4.25 Experiment in applying machine learning algorithms to predict the occurrence of PM_{2.5} caused LVDs

~~The severe and frequent LVDs or haze events due to particulate pollution have brought a serious issue to Southeast Asian countries in recent decades, interrupting working and school schedules, transportation, and outdoor activities alongside causing human health issues that all lead to economic loss. One measure to minimize such economic loss is to provide reliable forecasts for the occurrence of LVDs to allow corresponding mitigations be implemented beforehand.~~

Traditional physical models such as WRF-Chem are developed based on equations describing fluid dynamics, physical processes, and chemical reactions, and mass conservation equations to link these processes on different scales and to predict consequences resulting from circulation and physiochemical process evolutions. However, various parameterizations, and numerical as well as input data errors can all lead to the uncertainty of model prediction. Specifically, for the task of forecasting the occurrence of haze events (i.e., LVDs), using these models is nearly impossible due to the lack of real-time emission estimates to drive aerosol chemical and physical processes. On the other hand, ~~Machine Learning (ML)~~machine learning algorithms permit interpretation of large quantity of complex historical data based on computer analyses, and this capacity of ~~ML~~machine learning seems promising for us to derive suitable conditions for hazes from historical data and hence to forecast the likelihood of the occurrence of such events.

~~Here, we~~We hence experiment using the so-called supervised learning skill that trains or optimizes a machine to produce the outcomes based on input data (or features) as close as possible to known results, or gaining an accuracy as high as possible. In our experiment, we

585 have applied 6 different [ML-machine learning](#) algorithms, including Nearest Neighbors
586 (Pedregosa et al., 2011), Linear Support Vector Machine (SVM) (Schölkopf and Smola,
587 2002), SVM with Radial Basis Function Kernel (non-linear SVM) (Scholkopf et al., 1997;
588 Quinlan, 1986), Decision Tree (Quinlan, 1986), Random Forest (Breiman, 2001), and
589 Neural Network (Haykin et al., 2009), to reproduce past visibility patterns or to predict haze
590 occurrence. Through the supervised learning procedure, we have also examined the
591 importance of each input variable. These [ML-machine learning](#) machines are trained for
592 predicting LVDs at three airports in Singapore reporting to the GSOD, i.e., Changi, Seletar,
593 and Paya Labar. All the input data or features are listed in Table [S3S5](#). Data are available
594 from 2000 to 2015 at Changi and Paya Labar but only between 2004 and 2015 at Seletar.

595 We have used several different classifications in the training. The first one uses two
596 classes, corresponding to haze (visibility lower or equal to 10 km) and non-haze (visibility
597 higher than 10 km) events. Another applied 2-class classification uses 7 km instead of 10
598 km in identifying the haze events. In addition, a 3-class classification has also been tested,
599 which includes two haze classes: visibility ~~lower~~[lowers](#) than 7 km and between 10 and 7 km,
600 respectively. The training-testing ratio ~~was~~[is](#) set to be 60:40.

601 In ~~comparis~~[our study](#), the highest validation accuracy and F₁-score (Powers, 2011) in
602 any algorithm appear in the machine for Changi site, while the difference in accuracy
603 between each algorithm is small (Figs. [87](#) and [9S5](#)). However, the accuracy for ~~each~~
604 [algorithm](#)~~all the algorithms~~ at Seletar and Paya Labar drops dramatically by about 20-30%
605 in 2-class classification using 10-km visibility and 3-class classification. The reason for the
606 best performances in Changi is likely to be the least frequency of haze events at this site
607 (account for only 10% of the total LVDs), in comparison, 37% and 44% of haze events
608 occurred at Paya Labar and Seletar during the training time period, respectively. The

609 ~~model~~machines also ~~predicts~~predict non-haze events with higher accuracy than haze events
610 at Changi. Using severe haze (visibility < 7 km) instead of moderate haze (visibility < 10
611 km) to label haze event can also increase accuracy (over 80%). This could be due to [the fact](#)
612 that severe haze events are primarily caused by heavy biomass burnings, whose occurrence
613 would be well captured in the satellite hotspot input data.

614 Besides accuracy and F₁-score analysis, we have also used the *feature importance*
615 function in [the scikit-learn](#) Random Forest package to measure the importance of various
616 features (i.e. Gini importance) (Pedregosa et al., 2011). The function takes array of features
617 and computes the normalized total reduction of the criterion brought by that feature. The
618 higher the value, the more important the feature is to the forecasting machine. We find that
619 the hotspot counts from three fire regions are ranked consistently among the top three most
620 important features for most [model](#)machine learning predictions in all three classifications
621 (Fig. [408](#); Fig. S6 and S7). The values of importance of hotspot counts are higher than 0.15.
622 Analysis also suggests that “Month” is among the top five most important features in all
623 ~~models~~machines, followed by wind direction and relative humidity (Fig. [408](#)), implying that
624 besides fire hotspot, seasonal monsoon wind patterns, wind-related weather conditions (i.e.,
625 SRV in Fig. [408](#)) are also important factors in forecasting the occurrence of haze events in
626 Singapore. In addition, relative humidity is a critical variable for visibility (i.e., growth of
627 hygroscopic particles can drastically enhance the light extinction). These results are
628 consistent with previous studies of haze events in Singapore (Reid et al., 2012; Lee et al.,
629 2017). ~~To our surprise, precipitation in the fire regions does not appear to have a significant~~
630 ~~impact on Singapore haze compared to other features. Nevertheless, previous works by Reid~~
631 ~~et al. (2012) and Lee et al. (2017) also suggested the relationships between fire hotspot~~
632 ~~appearance and certain weather phenomena particularly precipitation. Therefore, we are~~

633 [surprised that precipitation in the fire regions does not appear to be a significant feature for](#)
634 [predicting Singapore haze compared with other features in our current analysis.](#)

635 **5.6 Summary**

636 We have quantified the impacts of fire (emitted from biomass burning) and non-fire
637 (emitted from anthropogenic sources other than biomass burning) aerosols on air quality and
638 visibility degradation over Southeast Asia, by using WRF-Chem in three scenarios driven
639 respectively by aerosol emissions from: (a) fossil fuel burning only, (b) biomass burning
640 only, and (c) both fossil fuel and biomass burning. ~~Based on the~~[These model results from](#)
641 ~~these scenarios, we conclude~~[reveal that the major reason behind the occurrence](#)39% of
642 observed low visibility days (LVDs) in 50 ASEAN cities ~~is aerosols from non-fire~~
643 ~~anthropogenic sources (59%), while fire aerosols cause an additional 13% of LVDs (both~~
644 ~~alone and coexisting with non-fire aerosols) in these cities. Conversely, by considering~~
645 ~~aerosols emitted from fire alone, about 47% of observed LVDs can be explained, whereas~~
646 ~~adding non-fire aerosols adds an additional 25% of LVDs. Out of these results, model fails~~
647 ~~to capture about~~ [by either fossil fuel burning or biomass burning emissions alone when they](#)
648 [coexist, a further 20% by fossil fuel burning alone, a further 8% by biomass burning alone,](#)
649 [and a further 5% by a combination of fossil fuel burning and biomass burning. The](#)
650 [remaining](#) 28% of observed LVDs [low visibility days remain unexplained, likely due to](#)
651 [emissions sources that have not been accounted for.](#) Our results show that owing to the
652 economic growth in Southeast Asia, non-fire aerosols have become the major reason to
653 cause LVDs in most Southeast Asian cities. However, for certain cities including
654 Singapore, LVDs are likely caused by coexisting fire and non-fire aerosols. Hence, both fire
655 and non-fire emissions play important roles in visibility degradation in Southeast Asia.

Formatted: Italian (Italy)

656 Furthermore, we have also used air quality index or AQI derived from modeled 9-hr
657 O₃ and 24-hr PM_{2.5} to analyze the air quality of these 50 ASEAN cities. The results are
658 consistent with the visibility modeling and analysis, indicating that PM_{2.5} particles, primarily
659 those from non-fire emissions, are the major reason behind high AQI(PM_{2.5}) occurrence in
660 these Southeast Asian cities. In addition to non-fire PM_{2.5} stand-alone cases, coexisting fire
661 and non-fire PM_{2.5} jointly caused an increase of 11% in bad air quality events with moderate
662 polluted or unhealthy pollution levels (23% versus 34%). The premature mortality among
663 the analyzed ASEAN cities has increased from ~4110 in 2002 to ~6540 in 2008. Bangkok
664 (Thailand), Jakarta (Indonesia), and Hanoi (Vietnam) are the top three cities in our analysis
665 for premature mortality due to air pollution, with 10761080, 910, and 624620 premature
666 mortalities per year, respectively.

Formatted: Not Superscript/Subscript

667 We find the reason behind the model's miss-capturing of 28% observed LVDs averaged
668 over 50 ASEAN cities is largely due to a lack of inclusion of anthropogenic fugitive and
669 industrial as well as road dust from urban sources in the emission inventories used in this
670 study. Using filtered-PM_{2.5} chemical composition data from the SPARTAN stations in
671 Hanoi, Singapore, Bandung, and Manila to filledfill the missing aerosol components from
672 these excluded sources can drastically increase modelthe captured LVDs by the model in
673 these cities, for example, by 47% in Singapore. The improvement in LVD prediction is
674 especially substantial in non-fire aerosols alone cases (Type 2; from 5% to 25%) and
675 coexisting fire and non-fire aerosols cases (Type 4; from 14% to 40%). Including the
676 missing anthropogenic dustsaerosols in modeled results also increases the occurrence of
677 cases with moderate and unhealthy air pollution levels from 22% to 66% in Singapore. Our
678 study clearly demonstrates the importance of anthropogenic dustsaerosols along with other

679 fugitive industrial and urban sources in air quality and visibility degradation in certain
680 Southeast Asian cities such as Singapore.

681 We have also experimented using [six different](#) machine learning algorithms to predict
682 the occurrence of LVDs caused by PM_{2.5}. ~~Six different machine learning algorithms have
683 been applied, including Nearest Neighbors, Linear Support Vector Machine (SVM), SVM
684 with Radial Basis Function Kernel (non-linear SVM), Decision Tree, Random Forest, and
685 Neural Network.~~—The effort is on forecasting hazes in three [GSODsurface visibility
686 observation](#) sites in Singapore. We find that the machine learning algorithms can predict
687 severe haze events (visibility < 7 km) with an accuracy greater than 80% in any [station-of
688 these stations](#). On the other hand, the accuracy is found to be sensitive to the selection of
689 features, labelling of outcome, and forecast sites.

690 The current study extends our previous effort (Lee et al., 2017) by using a model
691 including a full chemistry and aerosol package instead of a smoke aerosol module without
692 chemistry. The added model capacity provides more complete quantitative description of
693 physiochemical processes that allow us to better analyze the contribution of fire versus non-
694 fire aerosols to the regional air quality and visibility degradation. Our results show that the
695 majority of the population in Southeast Asian cities are exposed to air pollution that can be
696 mostly attributed to non-fire aerosols. On the other hand, our analysis also suggests that for
697 certain cities such as Singapore, severe air pollution are likely caused by coexisting fire and
698 non-fire aerosols. All these further complicate the options for air pollution mitigation.

699 **[67](#) Data availability**

700 FINNv1.5 emission data are publicly available from
701 <http://bai.acom.uar.edu/Data/fire/>. REAS and EDGAR emission data can be

702 downloaded from <https://www.nies.go.jp/REAS/> and
703 <http://edgar.jrc.ec.europa.eu/overview.php?v=42>, respectively. Malaysia API records
704 can be obtained from http://apims.doe.gov.my/public_v2/home.html. The observational
705 visibility from the GSOD can be downloaded from [https://data.noaa.gov/dataset/global-](https://data.noaa.gov/dataset/global-surface-summary-of-the-day-gsod)
706 [surface-summary-of-the-day-gsod](https://data.noaa.gov/dataset/global-surface-summary-of-the-day-gsod). CO and O₃ in WHO GAW station can be obtained
707 from <http://ds.data.jma.go.jp/gmd/wdcgg/>. Fine particle data from SPARTAN are
708 publicly available in <http://spartan-network.weebly.com/>. WRF-Chem simulated data are
709 available upon request from Hsiang-He Lee (hsiang-he@smart.mit.edu).

710

711 **Acknowledgements**

712 This research was supported by the National Research Foundation Singapore through the
713 Singapore-MIT Alliance for Research and Technology, the interdisciplinary research
714 program of Center for Environmental Sensing and Modeling. It was also supported by the
715 U.S. National Science Foundation (AGS-1339264) and U.S. Department of Energy (DE-
716 FG02-94ER61937). The authors thank MIT Greater China Fund for Innovation 2015 for
717 facilitating the collaboration between the Chinese University of Hong Kong and MIT
718 research teams. The authors would like to acknowledge the Ministry of Natural Resources
719 and Environment, Department of Environment, Malaysia for making Malaysia Air Pollution
720 Index data available; the World Meteorology Organization (WMO) Global Atmosphere
721 Watch (GAW) station Bukit Kototabang, SPARTAN, NCEP-FNL, and NCAR FINN
722 working groups for releasing their data to the research communities; and the NCAR WRF
723 developing team for providing the numerical model for this study. The computational work
724 for this article was performed on resources of the National Supercomputing Centre,
725 Singapore (<https://www.nsc.sg>).

Formatted: Font: +Body (Cambria), English (United States)

726
727
728

729 **References**

- 730 Ackermann, I. J., Hass, H., Memmesheimer, M., Ebel, A., Binkowski, F. S., and Shankar, U.:
731 Modal aerosol dynamics model for Europe: development and first applications,
732 Atmospheric Environment, 32, 2981-2999, [http://dx.doi.org/10.1016/S1352-](http://dx.doi.org/10.1016/S1352-2310(98)00006-5)
733 [2310\(98\)00006-5](http://dx.doi.org/10.1016/S1352-2310(98)00006-5), 1998.
- 734 [Benjamini, Y., and Hochberg, Y.: Controlling the False Discovery Rate: A Practical and](#)
735 [Powerful Approach to Multiple Testing, Journal of the Royal Statistical Society-](#)
736 [Series B \(Methodological\), 57, 289-300, 1995.](#)
- 737 [Berg, P., Moseley, C., and Haerter, J. O.: Strong increase in convective precipitation in](#)
738 [response to higher temperatures, Nature Geosci, 6, 181-185,](#)
739 [http://www.nature.com/ngeo/journal/v6/n3/abs/ngeo1731.html-](http://www.nature.com/ngeo/journal/v6/n3/abs/ngeo1731.html-supplementary-information)
740 [supplementary information, 2013.](http://www.nature.com/ngeo/journal/v6/n3/abs/ngeo1731.html-supplementary-information)
- 741 BPS: Statistik Indonesia-Statistical Yearbook of Indonesia, Badan Pusat Statistik, 2009.
- 742 Breiman, L.: Random Forests, Machine Learning, 45, 5-32, 10.1023/A:1010933404324,
743 2001.
- 744 Burnett, R. T., Pope III, C. A., Ezzati, M., Olives, C., Lim, S. S., Mehta, S., Shin, H. H., Singh,
745 G., Hubbell, B., and Brauer, M.: An integrated risk function for estimating the
746 global burden of disease attributable to ambient fine particulate matter
747 exposure, Environmental health perspectives, 122, 397, 2014.
- 748 Chen, T.-M., Kuschner, W. G., Gokhale, J., and Shofer, S.: Outdoor air pollution: ozone
749 health effects, The American journal of the medical sciences, 333, 244-248,
750 2007.
- 751 Crippa, P., Castruccio, S., Archer-Nicholls, S., Lebron, G. B., Kuwata, M., Thota, A., Sumin,
752 S., Butt, E., Wiedinmyer, C., and Spracklen, D. V.: Population exposure to
753 hazardous air quality due to the 2015 fires in Equatorial Asia, Scientific Reports,
754 6, 37074, 10.1038/srep37074, 2016.
- 755 CSOM: Statistical Yearbook 2010, The Government of the Republic of the Union of
756 Myanmar, 2010.
- 757 DSM: Population distribution and basic demographic characteristics, Department of
758 Statistics, Malaysia, Malaysia, 2010.
- 759 DSS: Singapore's Resident Population, 2003-2007, Department of Statistics Singapore,
760 Singapore, 2008.
- 761 DSS: Population Trends 2016, Department of Statistics Singapore, Singapore, 2016.
- 762 Frankenber, E., McKee, D., and Thomas, D.: Health consequences of forest fires in
763 Indonesia, Demography, 42, 109-129, 10.1353/dem.2005.0004, 2005.
- 764 [Grell, G. A., and Freitas, S. R.: A scale and aerosol aware stochastic convective](#)
765 [parameterization for weather and air quality modeling. Atmos. Chem. Phys., 14,](#)
766 [5233-5250, 10.5194/acp-14-5233-2014, 2014.](#)

767 GSOV: Population and Employment, General Statistics Office Of Vietnam, 2009.
768 Gu, Y., and Yim, S. H. L.: The air quality and health impacts of domestic trans-boundary
769 pollution in various regions of China, *Environment International*, 97, 117-124,
770 <http://dx.doi.org/10.1016/j.envint.2016.08.004>, 2016.
771 Haykin, S. S., Haykin, S. S., Haykin, S. S., and Haykin, S. S.: *Neural networks and learning*
772 *machines*, Pearson Upper Saddle River, NJ, USA; 2009.
773 [Iacono, M. J., Delamere, J. S., Mlawer, E. J., Shephard, M. W., Clough, S. A., and Collins, W.](https://doi.org/10.1029/2008JD009944)
774 [D.: Radiative forcing by long-lived greenhouse gases: Calculations with the AER](https://doi.org/10.1029/2008JD009944)
775 [radiative transfer models, *Journal of Geophysical Research: Atmospheres*, 113,](https://doi.org/10.1029/2008JD009944)
776 [n/a-n/a. 10.1029/2008JD009944, 2008.](https://doi.org/10.1029/2008JD009944)
777 IEA: Energy and Climate Change, World Energy Outlook Special Report, International
778 Energy Agency, pp. 74 -77, 2015.
779 Janssens-Maenhout, G., Crippa, M., Guizzardi, D., Dentener, F., Muntean, M., Pouliot, G.,
780 Keating, T., Zhang, Q., Kurokawa, J., Wankmüller, R., Denier van der Gon, H.,
781 Kuenen, J. J. P., Klimont, Z., Frost, G., Darras, S., Koffi, B., and Li, M.: HTAP_v2.2: a
782 mosaic of regional and global emission grid maps for 2008 and 2010 to study
783 hemispheric transport of air pollution, *Atmos. Chem. Phys.*, 15, 11411-11432,
784 10.5194/acp-15-11411-2015, 2015.
785 Kiehl, J. T., Schneider, T. L., Rasch, P. J., Barth, M. C., and Wong, J.: Radiative forcing due
786 to sulfate aerosols from simulations with the National Center for Atmospheric
787 Research Community Climate Model, Version 3, *Journal of Geophysical*
788 *Research: Atmospheres*, 105, 1441-1457, 10.1029/1999JD900495, 2000.
789 Klimont, Z., Kupiainen, K., Heyes, C., Purohit, P., Cofala, J., Rafaj, P., Borcken-Kleefeld, J.,
790 and Schöpp, W.: Global anthropogenic emissions of particulate matter including
791 black carbon, *Atmos. Chem. Phys. Discuss.*, 2016, 1-72, 10.5194/acp-2016-880,
792 2016.
793 Kunii, O., Kanagawa, S., Yajima, I., Hisamatsu, Y., Yamamura, S., Amagai, T., and Ismail, I.
794 T. S.: The 1997 Haze Disaster in Indonesia: Its Air Quality and Health Effects,
795 *Archives of Environmental Health: An International Journal*, 57, 16-22,
796 10.1080/00039890209602912, 2002.
797 Kurokawa, J., Ohara, T., Morikawa, T., Hanayama, S., Janssens-Maenhout, G., Fukui, T.,
798 Kawashima, K., and Akimoto, H.: Emissions of air pollutants and greenhouse
799 gases over Asian regions during 2000–2008: Regional Emission inventory in
800 ASia (REAS) version 2, *Atmos. Chem. Phys.*, 13, 11019-11058, 10.5194/acp-13-
801 11019-2013, 2013.
802 Lee, H. H., Bar-Or, R. Z., and Wang, C.: Biomass burning aerosols and the low-visibility
803 events in Southeast Asia, *Atmos. Chem. Phys.*, 17, 965-980, 10.5194/acp-17-
804 965-2017, 2017.
805 Li, Y., Henze, D. K., Jack, D., Henderson, B. H., and Kinney, P. L.: Assessing public health
806 burden associated with exposure to ambient black carbon in the United States,
807 *Science of The Total Environment*, 539, 515-525,
808 <https://doi.org/10.1016/j.scitotenv.2015.08.129>, 2016.
809 Lim, S. S., Vos, T., Flaxman, A. D., Danaei, G., Shibuya, K., Adair-Rohani, H., AlMazroa, M.
810 A., Amann, M., Anderson, H. R., and Andrews, K. G.: A comparative risk
811 assessment of burden of disease and injury attributable to 67 risk factors and
812 risk factor clusters in 21 regions, 1990–2010: a systematic analysis for the
813 Global Burden of Disease Study 2010, *The lancet*, 380, 2224-2260, 2013.

814 Malaysia, D. o. E.: A Guide To Air Pollutant Index in Malaysia, 4 ed., edited by: Malaysia,
815 D. o. E., 18 pp., 2000.

816 Marlier, M. E., DeFries, R. S., Voulgarakis, A., Kinney, P. L., Randerson, J. T., Shindell, D.
817 T., Chen, Y., and Faluvegi, G.: El Nino and health risks from landscape fire
818 emissions in southeast Asia, *Nature Clim. Change*, 3, 131-136,
819 [http://www.nature.com/nclimate/journal/v3/n2/abs/nclimate1658.html -
820 supplementary-information](http://www.nature.com/nclimate/journal/v3/n2/abs/nclimate1658.html-supplementary-information), 2013.

821 Miettinen, J., Shi, C., and Liew, S. C.: Deforestation rates in insular Southeast Asia
822 between 2000 and 2010, *Global Change Biology*, 17, 2261-2270,
823 10.1111/j.1365-2486.2011.02398.x, 2011.

824 [Mlawer, E. J., Taubman, S. J., Brown, P. D., Iacono, M. J., and Clough, S. A.: Radiative
825 transfer for inhomogeneous atmospheres: RRTM, a validated correlated-k
826 model for the longwave. *Journal of Geophysical Research: Atmospheres*, 102,
827 16663-16682, 10.1029/97JD00237, 1997.](#)

828 [Morrison, H., Thompson, G., and Tatarskii, V.: Impact of Cloud Microphysics on the
829 Development of Trailing Stratiform Precipitation in a Simulated Squall Line:
830 Comparison of One- and Two-Moment Schemes. *Monthly Weather Review*, 137,
831 991-1007, 10.1175/2008mwr2556.1, 2009.](#)

832 [Nakanishi, M., and Niino, H.: Development of an Improved Turbulence Closure Model
833 for the Atmospheric Boundary Layer. *Journal of the Meteorological Society of
834 Japan. Ser. II*, 87, 895-912, 10.2151/jmsj.87.895, 2009.](#)

835 National Centers for Environmental Prediction, N. W. S. N. U. S. D. o. C.: NCEP FNL
836 Operational Model Global Tropospheric Analyses, continuing from July 1999,
837 10.5065/D6M043C6, 2000.

838 NISC: Cambodia Inter-censal Population Survey 2013-Final Report, National Institute
839 of Statistics, Ministry of Planning, Phnom Penh, Cambodia, 2013.

840 NSCB: 2009 Philippine Statistical Yearbook, National Statistical Coordination Board,
841 Philippine 2009.

842 NSOT: Population and Housing Census 2010, National Statistical Office of Thailand,
843 2010.

844 Olivier, J., Van Aardenne, J., Dentener, F., Ganzeveld, L., and JAHW, P.: Recent trends in
845 global greenhouse gas emissions: regional trends and spatial distribution of key
846 sources.(169Kb) In:" Non-CO 2 Greenhouse Gases (NCGG-4)", A. van Amstel
847 (coord.), Millpress, Rotterdam, ISBN, 90, 043, 2005.

848 Pedregosa, F., Varoquaux, G., Gramfort, A., Michel, V., Thirion, B., Grisel, O., Blondel, M.,
849 Prettenhofer, P., Weiss, R., and Dubourg, V.: Scikit-learn: Machine learning in
850 Python, *Journal of Machine Learning Research*, 12, 2825-2830, 2011.

851 Philip, S., Martin, R. V., Snider, G., Weagle, C. L., Donkelaar, A. v., Brauer, M., Henze, D. K.,
852 Klimont, Z., Venkataraman, C., Sarath, K. G., and Zhang, Q.: Anthropogenic
853 fugitive, combustion and industrial dust is a significant, underrepresented fine
854 particulate matter source in global atmospheric models, *Environmental
855 Research Letters*, 12, 044018, 2017.

856 Powers, D. M.: Evaluation: from precision, recall and F-measure to ROC, informedness,
857 markedness and correlation, *Journal of Machine Learning Technologies*, 2, 37-
858 63, 2011.

859 Quinlan, J. R.: Induction of decision trees, *Machine learning*, 1, 81-106, 1986.

860 Reid, J. S., Xian, P., Hyer, E. J., Flatau, M. K., Ramirez, E. M., Turk, F. J., Sampson, C. R.,
861 Zhang, C., Fukada, E. M., and Maloney, E. D.: Multi-scale meteorological
862 conceptual analysis of observed active fire hotspot activity and smoke optical
863 depth in the Maritime Continent, *Atmos. Chem. Phys.*, 12, 2117-2147,
864 10.5194/acp-12-2117-2012, 2012.

865 Schell, B., Ackermann, I. J., Hass, H., Binkowski, F. S., and Ebel, A.: Modeling the
866 formation of secondary organic aerosol within a comprehensive air quality
867 model system, *Journal of Geophysical Research: Atmospheres* (1984–2012),
868 106, 28275-28293, 2001.

869 Scholkopf, B., Sung, K.-K., Burges, C. J., Girosi, F., Niyogi, P., Poggio, T., and Vapnik, V.:
870 Comparing support vector machines with Gaussian kernels to radial basis
871 function classifiers, *IEEE transactions on Signal Processing*, 45, 2758-2765,
872 1997.

873 Schölkopf, B., and Smola, A. J.: *Learning with kernels: support vector machines,*
874 *regularization, optimization, and beyond*, MIT press, 2002.

875 Smith, A., Lott, N., and Vose, R.: The Integrated Surface Database: Recent Developments
876 and Partnerships, *Bulletin of the American Meteorological Society*, 92, 704-708,
877 doi:10.1175/2011BAMS3015.1, 2011.

878 Snider, G., Weagle, C. L., Martin, R. V., van Donkelaar, A., Conrad, K., Cunningham, D.,
879 Gordon, C., Zwicker, M., Akoshile, C., Artaxo, P., Anh, N. X., Brook, J., Dong, J.,
880 Garland, R. M., Greenwald, R., Griffith, D., He, K., Holben, B. N., Kahn, R., Koren, I.,
881 Lagrosas, N., Lestari, P., Ma, Z., Vanderlei Martins, J., Quel, E. J., Rudich, Y., Salam,
882 A., Tripathi, S. N., Yu, C., Zhang, Q., Zhang, Y., Brauer, M., Cohen, A., Gibson, M. D.,
883 and Liu, Y.: SPARTAN: a global network to evaluate and enhance satellite-based
884 estimates of ground-level particulate matter for global health applications,
885 *Atmos. Meas. Tech.*, 8, 505-521, 10.5194/amt-8-505-2015, 2015.

886 Snider, G., Weagle, C. L., Murdymootoo, K. K., Ring, A., Ritchie, Y., Stone, E., Walsh, A.,
887 Akoshile, C., Anh, N. X., Balasubramanian, R., Brook, J., Qonitan, F. D., Dong, J.,
888 Griffith, D., He, K., Holben, B. N., Kahn, R., Lagrosas, N., Lestari, P., Ma, Z., Misra,
889 A., Norford, L. K., Quel, E. J., Salam, A., Schichtel, B., Segev, L., Tripathi, S., Wang,
890 C., Yu, C., Zhang, Q., Zhang, Y., Brauer, M., Cohen, A., Gibson, M. D., Liu, Y.,
891 Martins, J. V., Rudich, Y., and Martin, R. V.: Variation in global chemical
892 composition of PM_{2.5}: emerging results from SPARTAN, *Atmos. Chem. Phys.*, 16,
893 9629-9653, 10.5194/acp-16-9629-2016, 2016.

894 Stockwell, W. R., Kirchner, F., Kuhn, M., and Seefeld, S.: A new mechanism for regional
895 atmospheric chemistry modeling, *Journal of Geophysical Research:*
896 *Atmospheres*, 102, 25847-25879, 10.1029/97JD00849, 1997.

897 [Tewari, M., F. Chen, W. Wang, J. Dudhia, M. A. LeMone, K. Mitchell, M. Ek, G. Gayno, J.](#)
898 [Wegiel, and Cuenca, R. H.: Implementation and verification of the unified NOAA](#)
899 [land surface model in the WRF model, 20th conference on weather analysis and](#)
900 [forecasting/16th conference on numerical weather prediction. Seattle, WA,](#)
901 [U.S.A., 2004.](#)

902 van der Werf, G. R., Morton, D. C., DeFries, R. S., Olivier, J. G. J., Kasibhatla, P. S., Jackson,
903 R. B., Collatz, G. J., and Randerson, J. T.: CO₂ emissions from forest loss, *Nature*
904 *Geosci*, 2, 737-738,
905 http://www.nature.com/ngeo/journal/v2/n11/supinfo/ngeo671_S1.html,
906 2009.

907 Visscher, A. D.: Air Dispersion Modeling: Foundations and Applications, First ed., John
908 Wiley & Sons, Inc., 2013.

909 Wang, C.: A modeling study on the climate impacts of black carbon aerosols, Journal of
910 Geophysical Research: Atmospheres, 109, n/a-n/a, 10.1029/2003JD004084,
911 2004.

912 Wang, C.: Impact of direct radiative forcing of black carbon aerosols on tropical
913 convective precipitation, Geophysical Research Letters, 34,
914 10.1029/2006GL028416, 2007.

915 ~~Wang, C.: Anthropogenic aerosols and the distribution of past large-scale precipitation~~
916 ~~change, Geophysical Research Letters, 42, 10,876-810,884,~~
917 ~~10.1002/2015GL066416, 2015.~~

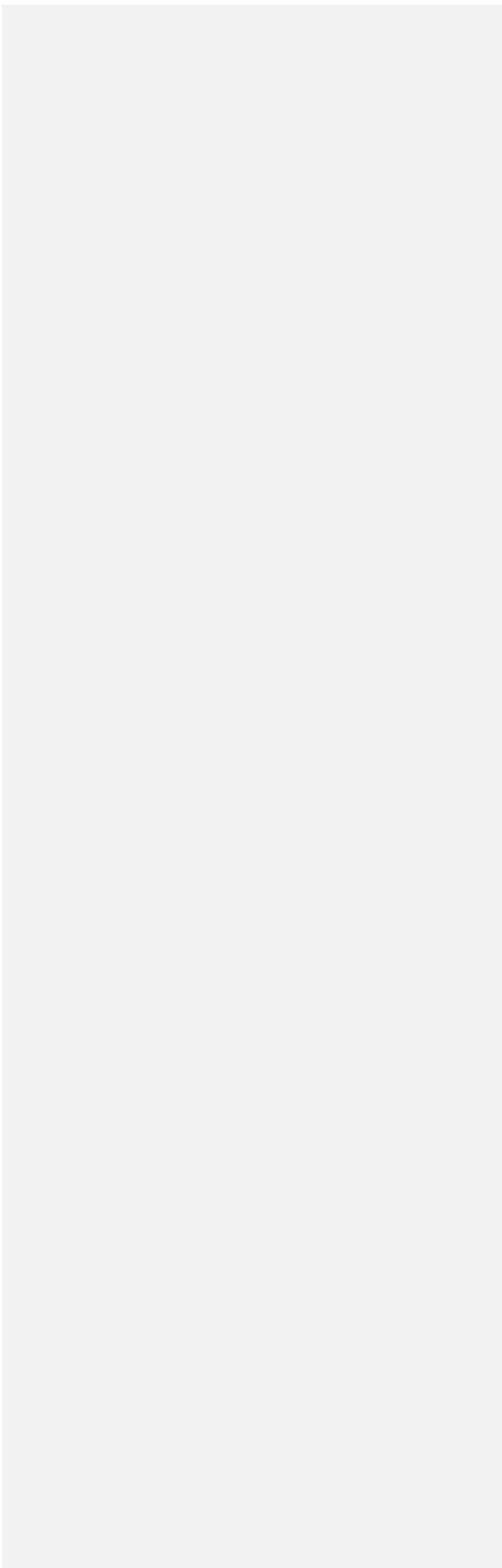
918 Wiedinmyer, C., Akagi, S. K., Yokelson, R. J., Emmons, L. K., Al-Saadi, J. A., Orlando, J. J.,
919 and Soja, A. J.: The Fire INventory from NCAR (FINN): a high resolution global
920 model to estimate the emissions from open burning, Geosci. Model Dev., 4, 625-
921 641, 10.5194/gmd-4-625-2011, 2011.

922 ~~Wilks, D. S.: "The Stippling Shows Statistically Significant Grid Points": How Research~~
923 ~~Results are Routinely Overstated and Overinterpreted, and What to Do about It,~~
924 ~~Bulletin of the American Meteorological Society, 97, 2263-2273,~~
925 ~~10.1175/BAMS-D-15-00267.1, 2016.~~

926
927

Formatted: Justified, Indent: Left: 0", Line spacing: single

028
029
030
031



032
033
034
035

Table 1. WRF physics scheme configuration

Physics Processes	Scheme
microphysics	Morrison (2 moments) scheme
longwave radiation	RRTMG scheme
shortwave radiation	RRTMG scheme
surface-layer	MYNN surface layer
land surface	Unified Noah land surface model
planetary boundary layer	MYNN 2.5 level TKE scheme
cumulus parameterization	Grell Freitas ensemble scheme

Formatted: Font +Body (Cambria)
Formatted: Font +Body (Cambria), Bold

936 **Table 2.** Mean annual emissions of BC, OC, SO₂, CO and NO₂ from biomass burning
 937 emission (BB; from FINN emission inventory) and fossil fuel burning emission (FF; from
 938 the combination of REAS and EDGAR emission inventories shown in Fig. 1) in the
 939 simulated domain from 2002 to 2008. Parentheses show the percentage of emission
 940 from fire and non-fire sources.
 941
 942

Formatted: Font: +Body (Cambria)

Formatted: Font: +Body (Cambria)

Formatted: Font: +Body (Cambria)

Units: Tg/yr	BC	OC	SO₂	CO	NO₂
BB	0.4 (50%)	4.1 (73%)	0.4 (7%)	71.6 (64%)	2.6 (37%)
FF	0.4 (50%)	1.4 (27%)	5.8 (93%)	39.9 (36%)	4.3 (63%)

943
944

045 Table 3. Comparison of the Air Quality Index (AQI) values with level of pollution index
 046 category and breakpoints for AQI derived from modeled 24 hr PM_{2.5} (µg m⁻³) and modeled
 047 9-hr O₃ (ppb).
 048

Index Category	AQI	24 hr PM _{2.5} (µg/m ³)	9-hr O ₃ (ppb)
Good	0–50	0.0–12.0	0–59
Moderate	51–100	12.1–35.4	60–75
Unhealthy	101–200	35.5–150.4	76–115
Very Unhealthy	201–300	150.5–250.4	116–374
Hazardous	301–400	250.5–350.4	†
Hazardous	401–500	350.5–500.4	†

049
 050

951 ~~Table 42~~. The contribution of fire aerosols (BB), non-fire aerosols (FF), or coexisting
 952 aerosols (~~FFBB~~) to low visibility days (LVDs) (based on the logic chart in Fig. 2) in
 953 Bangkok, Kuala Lumpur, Singapore, and among 50 Association of Southeast Asian Nations
 954 (ASEAN) cities during 2002-2008.

	Bangkok	Kuala Lumpur	Singapore	50 ASEAN cities
FF∩BB (Type 1)	22±10%	12±5%	3±4%	39±5%
FF (Type 2)	19±5%	16±16%	5±4%	20±3%
BB (Type 3)	19±7%	8±5%	11±13%	8±2%
FF+BB (Type 4)	11±4%	15±6%	14±8%	5±1%
Missing (Type 5)	29±5%	49±26%	67±21%	28±2%

956
 957

958 Table 53. The frequency of occurrence of air pollution level in Bangkok, Kuala Lumpur,
 959 Singapore, and 50 Association of Southeast Asian Nations (ASEAN) cities derived using 9-
 960 [Eq. 9-1](#) Ozone (O₃) volume mixing ratio in FF, BB, and FFBB during 2002-2008.
 961

Bangkok	AQI_(O3)	FF	BB	FFBB
Good	0-50	81±3%	97±1%	69±3%
Moderate	51-100	17±2%	3±1%	21±3%
Unhealthy	101-200	2±1%	0±0%	11±1%
Very Unhealthy	201-300	0±0%	0±0%	0±0%
Hazardous	301-400	0±0%	0±0%	0±0%
Hazardous	401-500	0±0%	0±0%	0±0%
Kuala Lumpur	AQI_(O3)	FF	BB	FFBB
Good	0-50	95±2%	100±1%	83±6%
Moderate	51-100	5±2%	0±1%	15±5%
Unhealthy	101-200	0±0%	0±0%	2±1%
Very Unhealthy	201-300	0±0%	0±0%	0±0%
Hazardous	301-400	0±0%	0±0%	0±0%
Hazardous	401-500	0±0%	0±0%	0±0%
Singapore	AQI_(O3)	FF	BB	FFBB
Good	0-50	99±1%	100±0%	94±3%
Moderate	51-100	1±1%	0±0%	5±2%
Unhealthy	101-200	0±0%	0±0%	1±1%
Very Unhealthy	201-300	0±0%	0±0%	0±0%
Hazardous	301-400	0±0%	0±0%	0±0%
Hazardous	401-500	0±0%	0±0%	0±0%
50 ASEAN cities	AQI_(O3)	FF	BB	FFBB
Good	0-50	94±1%	99±0%	88±2%
Moderate	51-100	6±1%	1±0%	10±2%
Unhealthy	101-200	0±0%	0±0%	2±0%
Very Unhealthy	201-300	0±0%	0±0%	0±0%
Hazardous	301-400	0±0%	0±0%	0±0%
Hazardous	401-500	0±0%	0±0%	0±0%

962
963

Table 64. Same as Table 53 but using 24-hr PM_{2.5} concentration.

Bangkok	AQI_(PM_{2.5})	FF	BB	FFBB
Good	0-50	63±6%	67±5%	38±2%
Moderate	51-100	34±5%	24±3%	45±3%
Unhealthy	101-200	3±2%	9±4%	17±4%
Very Unhealthy	201-300	0±0%	0±0%	0±0%
Hazardous	301-400	0±0%	0±0%	0±0%
Hazardous	401-500	0±0%	0±0%	0±0%
Kuala Lumpur	AQI_(PM_{2.5})	FF	BB	FFBB
Good	0-50	73±3%	78±8%	52±7%
Moderate	51-100	27±4%	18±6%	40±4%
Unhealthy	101-200	0±0%	4±3%	8±4%
Very Unhealthy	201-300	0±0%	0±0%	0±0%
Hazardous	301-400	0±0%	0±0%	0±0%
Hazardous	401-500	0±0%	0±0%	0±0%
Singapore	AQI_(PM_{2.5})	FF	BB	FFBB
Good	0-50	92±5%	92±4%	78±5%
Moderate	51-100	8±4%	6±2%	19±4%
Unhealthy	101-200	0±1%	1±2%	3±2%
Very Unhealthy	201-300	0±0%	0±0%	0±0%
Hazardous	301-400	0±0%	0±0%	0±0%
Hazardous	401-500	0±0%	0±0%	0±0%
50 ASEAN cities	AQI_(PM_{2.5})	FF	BB	FFBB
Good	0-50	77±1%	90±3%	66±3%
Moderate	51-100	19±1%	7±2%	26±2%
Unhealthy	101-200	4±0%	2±1%	8±2%
Very Unhealthy	201-300	0±0%	0±0%	0±0%
Hazardous	301-400	0±0%	0±0%	0±0%
Hazardous	401-500	0±0%	0±0%	0±0%

966

967 Table 75. The old (without missing anthropogenic dust aerosol components) and new (with
 968 missing anthropogenic dust aerosol components in FF and FFBB) calculated percentage of
 969 observed low visibility days (LVDs) ~~caused by defined aerosol types~~, categorized
 970 according the type classification explained in Fig. 2 ~~in Hanoi, Singapore, Bandung and~~
 971 Manila during 2002-2008.
 972

	Hanoi		Singapore		Bandung		Manila	
	old	new	old	new	old	new	old	new
FF∩BB (Type 1)	38±32%	40±31%	3±4%	5±7%	41±73%	41±74%	0±0%	1±1%
FF (Type 2)	34±8%	57±13%	5±4%	25±13%	8±19%	8±20%	3±3%	29±33%
BB (Type 3)	2±2%	0±0%	11±13%	9±10%	0±0%	0±0%	3±3%	2±3%
FF+BB (Type 4)	5±3%	1±1%	14±8%	40±19%	0±0%	0±0%	2±2%	11±3%
Missing (Type 5)	21±15%	2±4%	67±21%	20±9%	51±56%	51±57%	92±41%	57±16%

973
 974

975
 976
 977
 978
 979

Table 86. The frequency of various daily air pollution levels in Hanoi, Singapore, Bandung and Manila derived using 24-hr PM_{2.5} concentration with (new) and without (old) the missing anthropogenic dust/aerosol components in FFBB during 2002-2008.

Hanoi	AQI_(PM2.5)	old	new
Good	0-50	43±7%	0±0%
Moderate	51-100	46±3%	32±4%
Unhealthy	101-200	10±3%	67±4%
Very Unhealthy	201-300	0±0%	0±0%
Hazardous	301-400	0±0%	0±0%
Hazardous	401-500	0±0%	0±0%
Singapore	AQI_(PM2.5)	old	new
Good	0-50	78±5%	33±8%
Moderate	51-100	19±4%	59±8%
Unhealthy	101-200	3±2%	7±3%
Very Unhealthy	201-300	0±0%	0±0%
Hazardous	301-400	0±0%	0±0%
Hazardous	401-500	0±0%	0±0%
Bandung	AQI_(PM2.5)	old	new
Good	0-50	36±7%	0±0%
Moderate	51-100	58±5%	52±8%
Unhealthy	101-200	6±3%	48±8%
Very Unhealthy	201-300	0±0%	0±0%
Hazardous	301-400	0±0%	0±0%
Hazardous	401-500	0±0%	0±0%
Manila	AQI_(PM2.5)	old	new
Good	0-50	92±4%	64±5%
Moderate	51-100	7±3%	34±5%
Unhealthy	101-200	1±1%	2±1%
Very Unhealthy	201-300	0±0%	0±0%
Hazardous	301-400	0±0%	0±0%
Hazardous	401-500	0±0%	0±0%

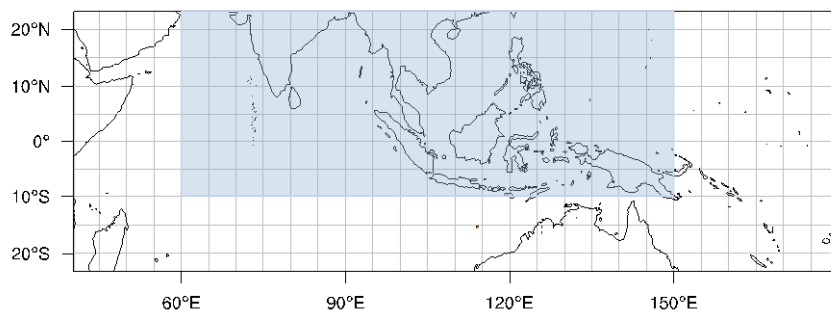
980

981 Table 97. Updated PM_{2.5} concentration ($\mu\text{g m}^{-3}$) and premature mortality (95% confidence
 982 intervals) in Hanoi, Singapore, Bandung and Manila with missing anthropogenic
 983 [aerosol components](#).

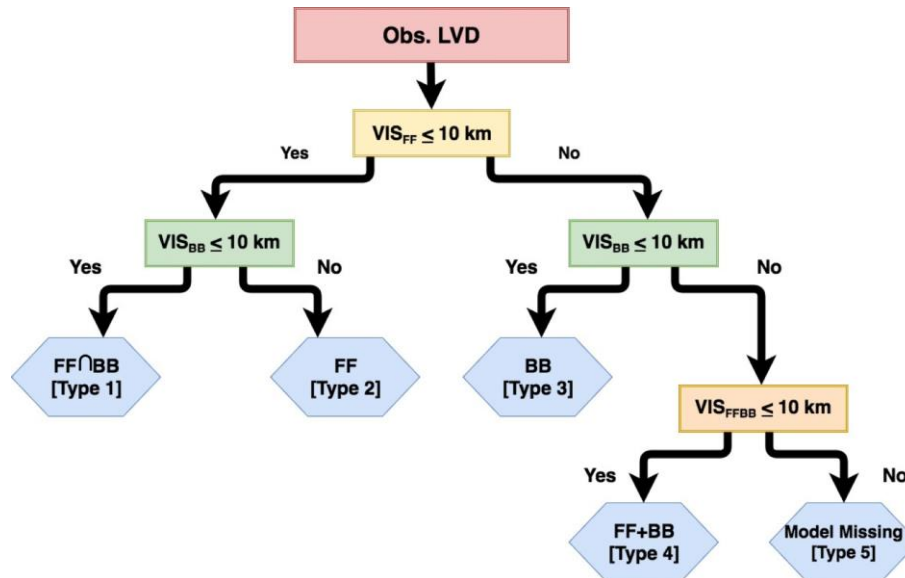
City	PM _{2.5} ($\mu\text{g m}^{-3}$)	Premature mortality
Hanoi	41.07	671 670 (210- 1841180)
Singapore	16.43	230 (22-55420-550)
Bandung	33.18	261 (65-481260 (70- 480)
Manila	12.38	128 (12130 (10-260)

985

986
987
988

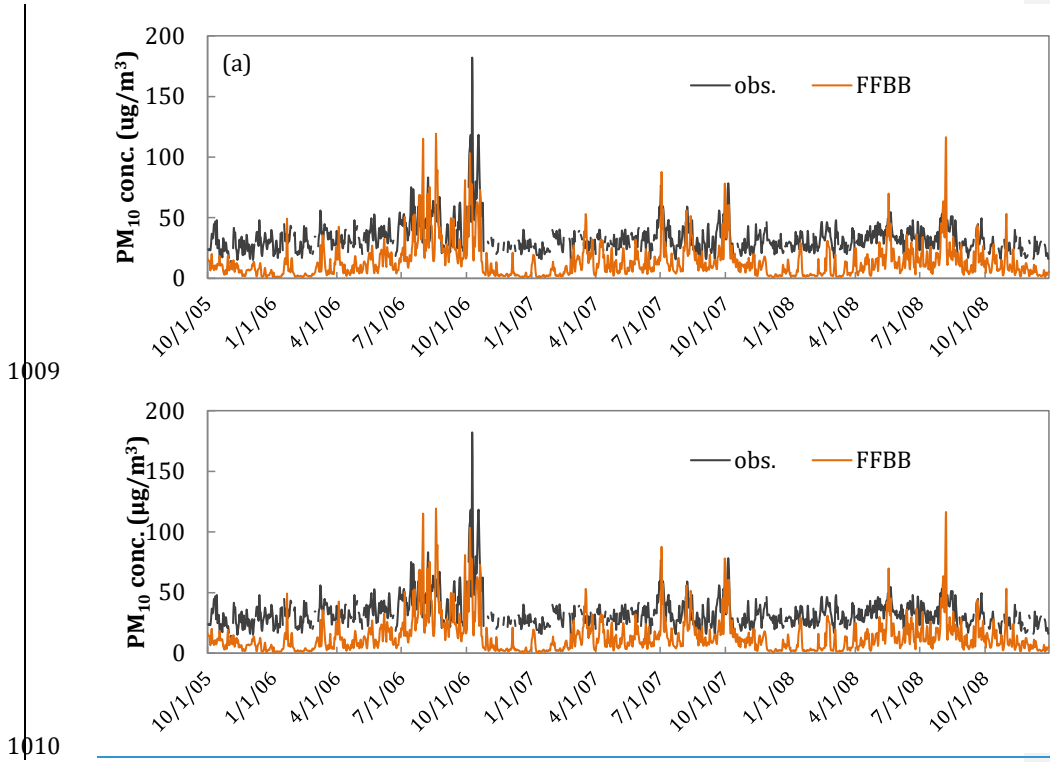


989
990 Figure 1. Model domain used for simulations. ~~Blue~~The blue color region indicates the fossil
991 fuel emission coverage from the Regional Emission inventory in ASia (REAS). The rest
992 of the domain uses the fossil fuel emission from the Emissions Database for Global
993 Atmospheric Research (EDGAR). ~~The domain has 432×148 grid points with a horizontal~~
994 ~~resolution of 36km.~~
995



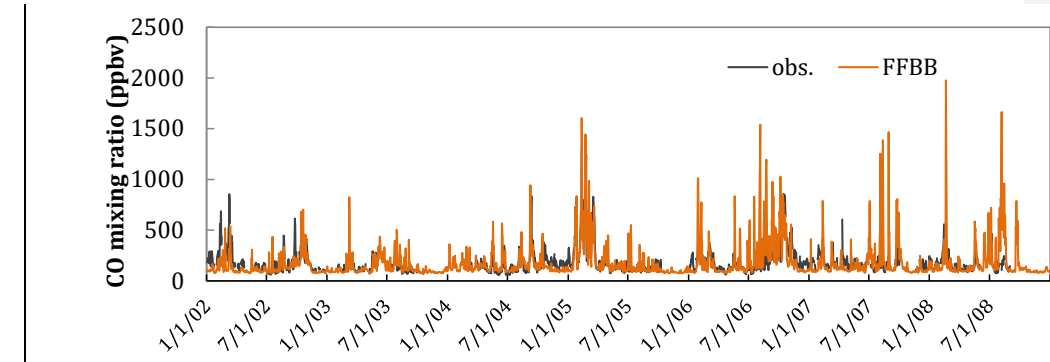
996
 997
 998
 999
 1000
 1001
 1002
 1003
 1004
 1005
 1006
 1007
 1008

Figure 2. Logical chart for fire (BB), non-fire (FF), or coexisting fire and non-fire (FF+BB) aerosols caused Low Visibility Day (LVD). “Obs. LVD” is an identified low visibility day from observation. Then, the modeled visibility from FF (VIS_{FF}), BB (VIS_{BB}), and FFBB (VIS_{FFBB}) are used to classify observed LVD into 5 types of LVD. Type 1 LVD represents the cases where either fire or non-fire aerosols alone can cause the observed LVD to occur. Type 2 means that non-fire aerosols are the major contributor to the observed LVD. Type 3 means that biomass-burning-fire aerosols are the major contributor to the observed LVD. Type 4 represents the cases where the observed LVD is induced by coexisting fire and non-fire aerosols. The observed LVDs that the model cannot capture are classified as Type 5.

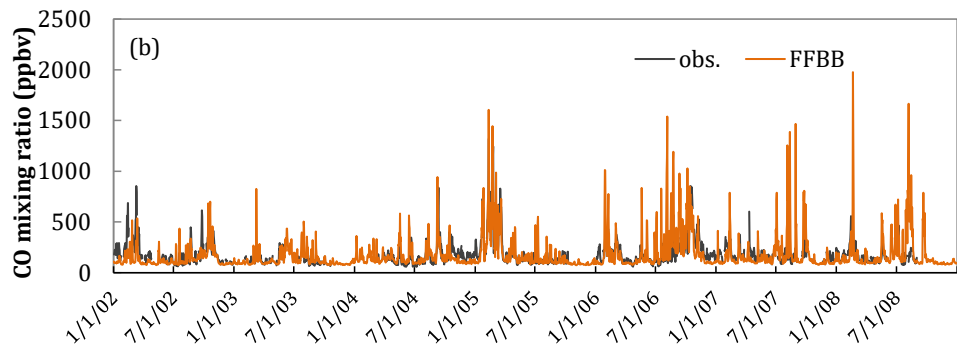


1009

1010

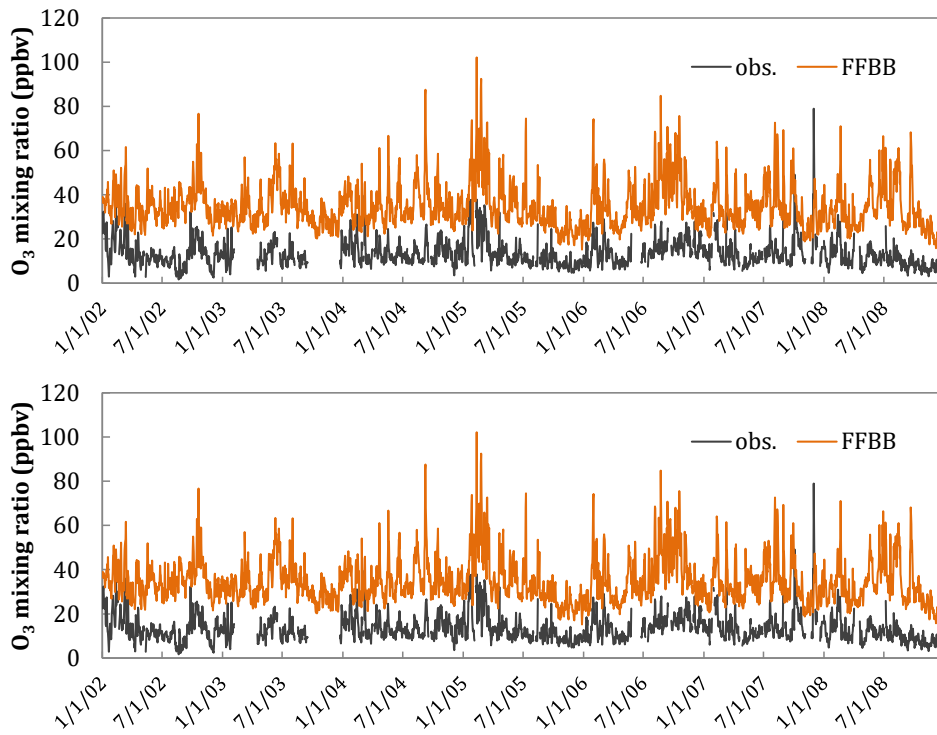


1011



1012

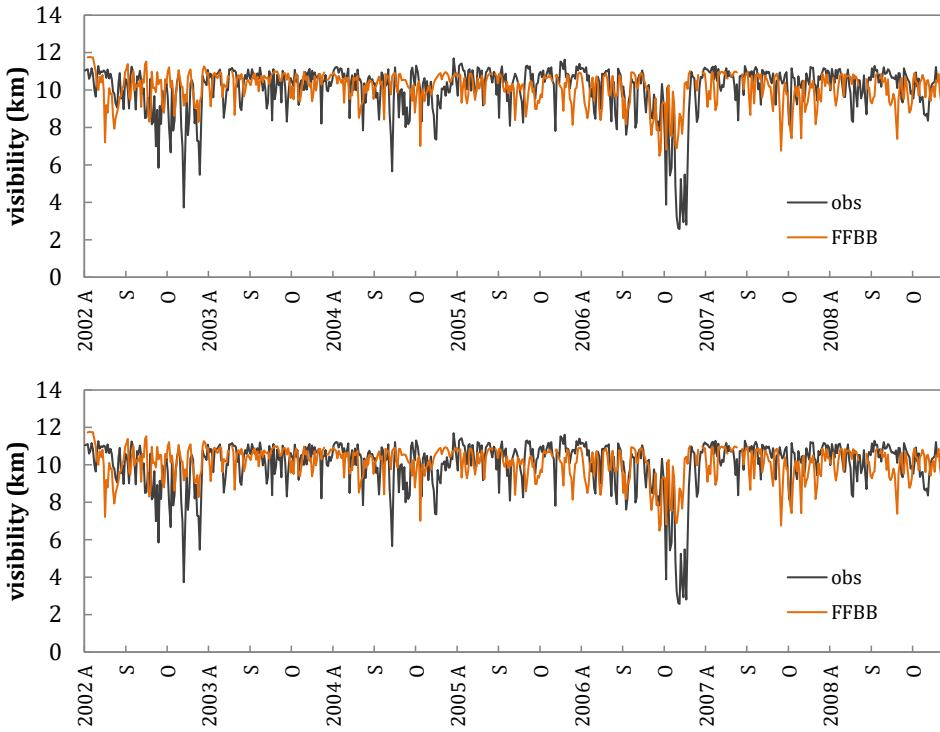
1013



1014

1015 Figure 3. (a) Time series of daily surface PM₁₀ ($\mu\text{g m}^{-3}$; AQI derived) from the ground-based
1016 observations (black line) and FFBB-simulated results (orange line) in Kuala Lumpur,
1017 Malaysia during October 2005 – December 2008. (b) Time series of daily surface CO
1018 mixing ratio (ppbv) from the ground-based observations (black line) and FFBB-simulated
1019 results (orange line) in Bukit Kototabang, Indonesia during 2002 – 2008. (c) Same as (b) but
1020 surface O₃.
1021

1022



1023

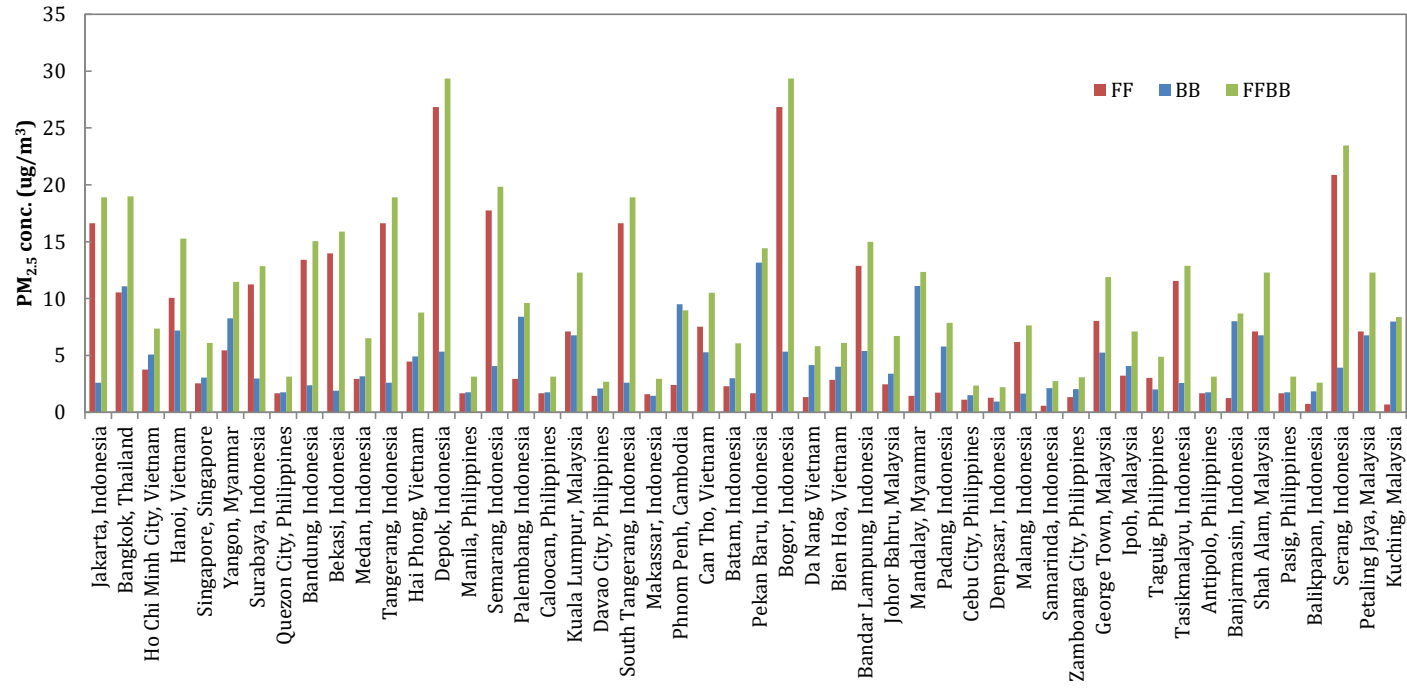
1024

1025

1026

1027

Figure 4. Comparison of daily visibility between GSOD observation (black line) and FFBB-simulated results (orange line) in Singapore during the fire seasons from 2002 to 2008. A, S, and O in the *x* axis indicates August, September, and October.



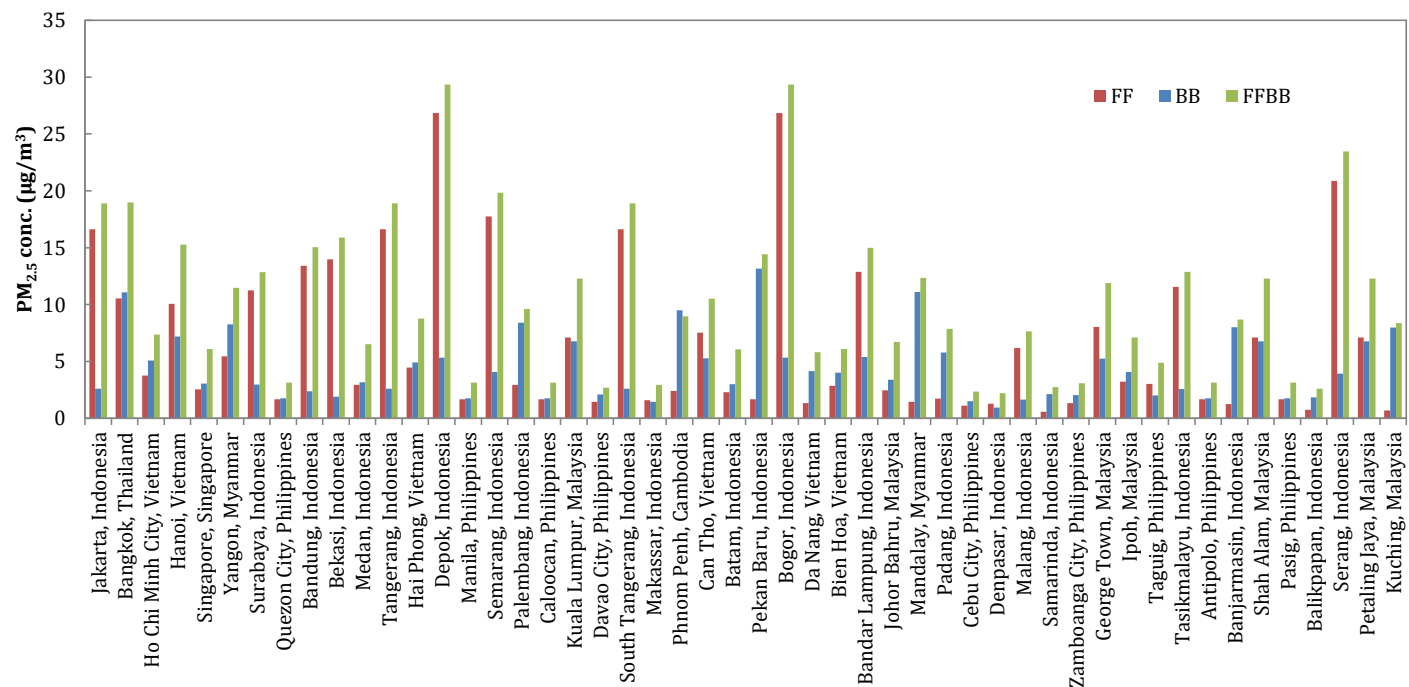
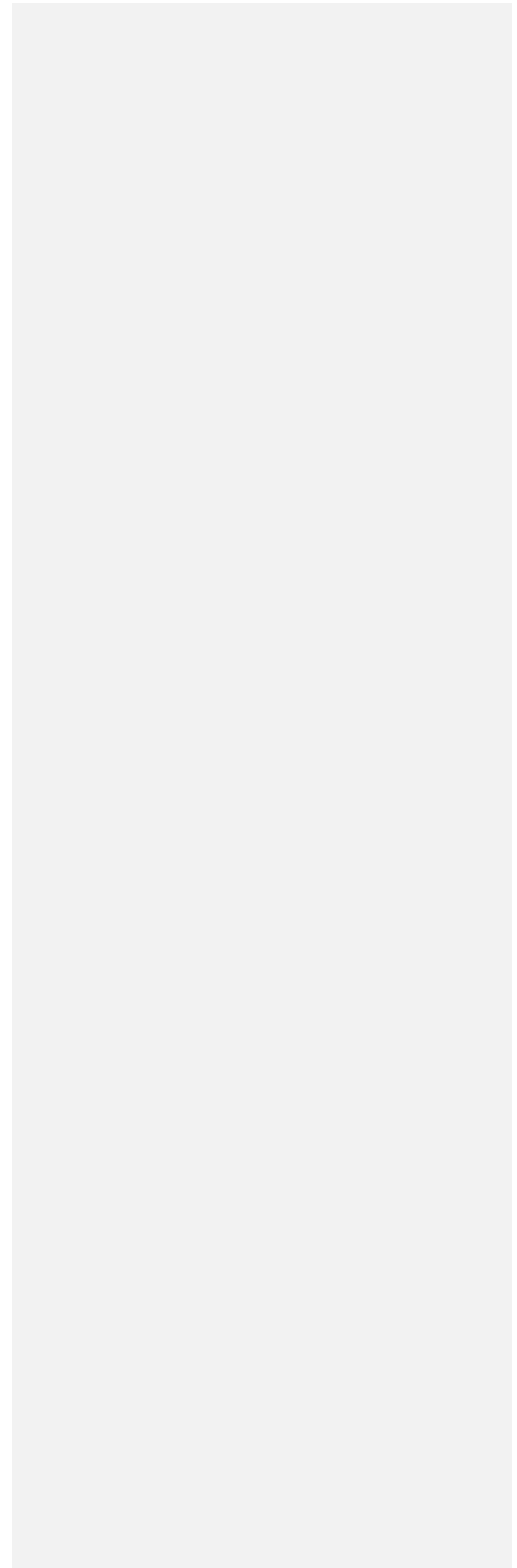


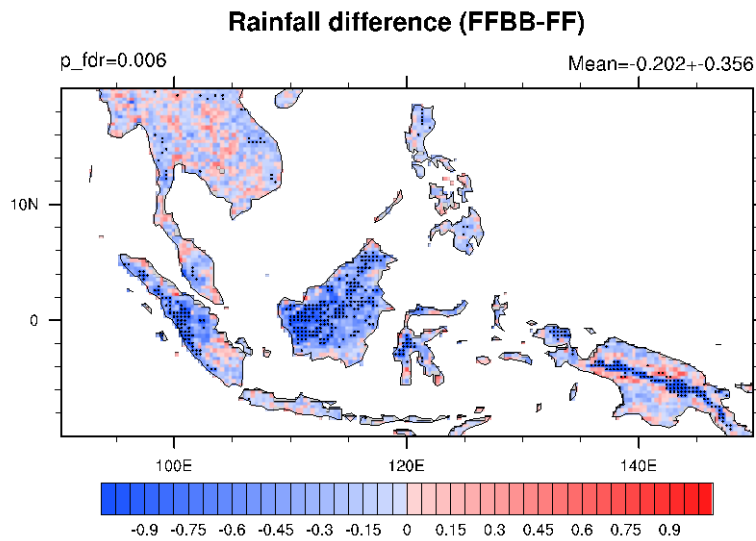
Figure 5. The annual mean simulated PM_{2.5} concentration ($\mu\text{g m}^{-3}$) in 50 Association of Southeast Asian Nations (ASEAN) cities, derived from FF (red), BB (blue), and FFBB (green) simulations and averaged over the period 2002-2008.

1029
1030
1031
1032
1033

Cities	Country	2002	2003	2004	2005	2006	2007	2008
Jakarta	Indonesia	850 (150-1660)	830 (130-1650)	900 (160-1750)	950 (180-1820)	910 (150-1790)	960 (170-1870)	970 (170-1900)
Bangkok	Thailand	850 (90-1950)	1010 (130-2230)	1030 (130-2280)	1170 (180-2530)	1120 (150-2480)	1180 (160-2590)	1170 (150-2650)
HoChiMinhCity	Vietnam	0 (0-0)	830 (0-1750)	810 (0-1590)	610 (0-1130)	0 (0-1180)	230 (0-1580)	0 (0-1530)
Hanoi	Vietnam	420 (40-880)	520 (80-1020)	540 (80-1060)	560 (90-1100)	570 (80-1120)	610 (100-1190)	1150 (190-2250)
Singapore	Singapore	0 (0-0)	0 (0-0)	0 (0-260)	0 (0-190)	0 (0-290)	0 (0-290)	0 (0-0)
Yangon	Myanmar	0 (0-380)	280 (20-630)	350 (30-730)	330 (30-710)	280 (20-640)	400 (40-820)	330 (20-730)
Surabaya	Indonesia	210 (30-440)	210 (20-430)	230 (30-460)	230 (30-470)	230 (30-470)	240 (30-480)	230 (20-480)
QuezonCity	Philippines	0 (0-0)	0 (0-0)	0 (0-0)	0 (0-0)	0 (0-0)	0 (0-0)	0 (0-0)
Bandung	Indonesia	200 (30-400)	200 (30-400)	210 (30-420)	230 (40-450)	200 (20-410)	220 (30-450)	220 (30-440)
Bekasi	Indonesia	150 (20-310)	160 (20-320)	180 (30-350)	190 (30-380)	190 (30-380)	210 (30-410)	210 (30-420)
Medan	Indonesia	0 (0-0)	0 (0-0)	0 (0-220)	10 (0-250)	0 (0-240)	0 (0-180)	0 (0-160)
Tangerang	Indonesia	120 (20-240)	120 (20-250)	140 (20-270)	150 (30-290)	150 (20-300)	170 (30-320)	170 (30-340)
HaiPhong	Vietnam	0 (0-0)	210 (10-450)	200 (0-480)	230 (10-510)	200 (0-500)	270 (30-580)	280 (30-590)
Depok	Indonesia	130 (30-230)	130 (30-250)	150 (30-270)	160 (40-300)	160 (40-310)	180 (40-330)	190 (40-350)
Manila	Philippines	0 (0-0)	0 (0-0)	0 (0-0)	0 (0-0)	0 (0-0)	0 (0-0)	0 (0-0)
Semarang	Indonesia	120 (20-240)	120 (20-240)	140 (30-260)	140 (30-280)	140 (30-280)	150 (30-290)	150 (30-300)
Palembang	Indonesia	100 (10-210)	0 (0-0)	100 (10-210)	0 (0-0)	150 (30-280)	0 (0-0)	0 (0-0)
Caloocan	Philippines	0 (0-0)	0 (0-0)	0 (0-0)	0 (0-0)	0 (0-0)	0 (0-0)	0 (0-0)
KualaLumpur	Malaysia	130 (10-290)	100 (0-260)	160 (20-340)	170 (20-360)	170 (20-360)	150 (10-340)	150 (10-340)
DavaoCity	Philippines	0 (0-0)	0 (0-0)	0 (0-0)	0 (0-0)	0 (0-0)	0 (0-0)	0 (0-0)
SouthTangerang	Indonesia	130 (20-250)	120 (20-240)	130 (20-250)	140 (30-260)	130 (20-250)	130 (20-260)	130 (20-260)
Makassar	Indonesia	0 (0-0)	0 (0-0)	0 (0-0)	0 (0-0)	0 (0-0)	0 (0-0)	0 (0-0)
PhnomPenh	Cambodia	0 (0-0)	0 (0-40)	40 (10-90)	30 (0-80)	30 (0-80)	40 (0-90)	40 (0-90)
CanTho	Vietnam	60 (0-270)	0 (10-310)	140 (20-170)	170 (20-360)	160 (10-350)	180 (20-380)	180 (20-380)
Batam	Indonesia	0 (0-0)	0 (0-0)	0 (0-50)	0 (0-60)	10 (0-80)	0 (0-90)	0 (0-0)
PekanBaru	Indonesia	70 (0-80)	0 (0-40)	60 (10-120)	80 (20-150)	80 (10-150)	70 (10-140)	70 (10-150)
Bogor	Indonesia	100 (20-180)	100 (20-180)	100 (20-190)	110 (30-200)	100 (20-200)	110 (30-200)	110 (30-210)
DaNang	Vietnam	0 (0-0)	0 (0-0)	90 (0-210)	0 (0-180)	0 (0-0)	0 (0-170)	0 (0-100)
BienHoa	Vietnam	0 (0-0)	0 (0-0)	60 (0-150)	0 (0-130)	0 (0-0)	0 (0-70)	0 (0-100)
BandarLampung	Indonesia	70 (10-140)	0 (10-140)	70 (10-140)	70 (10-140)	80 (10-160)	70 (10-150)	80 (10-160)
JohorBahru	Malaysia	0 (0-0)	0 (0-0)	20 (0-170)	0 (0-160)	60 (0-200)	0 (0-190)	0 (0-70)
Mandalay	Myanmar	0 (0-0)	290 (20-610)	330 (30-670)	300 (30-640)	300 (30-650)	360 (40-740)	340 (30-710)
Padang	Indonesia	0 (0-0)	0 (0-0)	0 (0-60)	0 (0-90)	0 (10-130)	0 (0-110)	0 (0-100)
CebuCity	Philippines	0 (0-0)	0 (0-0)	0 (0-0)	0 (0-0)	0 (0-0)	0 (0-0)	0 (0-0)
Denpasar	Indonesia	0 (0-0)	0 (0-0)	0 (0-0)	0 (0-0)	0 (0-0)	0 (0-0)	0 (0-0)
Malang	Indonesia	30 (0-100)	0 (0-50)	30 (0-100)	20 (0-100)	10 (0-100)	10 (0-100)	0 (0-100)
Samarinda	Indonesia	0 (0-0)	0 (0-0)	0 (0-0)	0 (0-0)	0 (0-0)	0 (0-0)	0 (0-0)
ZamboangaCity	Philippines	0 (0-0)	0 (0-0)	0 (0-0)	0 (0-0)	0 (0-0)	0 (0-0)	0 (0-0)
GeorgeTown	Malaysia	110 (10-250)	100 (10-240)	140 (10-290)	140 (10-290)	120 (10-270)	120 (10-260)	120 (10-270)
Ipoh	Malaysia	0 (0-0)	0 (0-0)	50 (0-120)	0 (0-120)	0 (0-90)	0 (0-50)	0 (0-90)
Taguig	Philippines	0 (0-0)	0 (0-0)	0 (0-60)	0 (0-90)	0 (0-0)	0 (0-0)	0 (0-0)
Tasikmalayu	Indonesia	30 (0-70)	30 (0-70)	40 (0-80)	40 (10-90)	40 (0-80)	50 (10-90)	50 (10-100)
Antipolo	Philippines	0 (0-0)	0 (0-0)	0 (0-0)	0 (0-0)	0 (0-0)	0 (0-0)	0 (0-0)
Banjarmasin	Indonesia	50 (10-100)	0 (0-0)	50 (10-110)	0 (0-0)	60 (10-110)	0 (0-0)	0 (0-0)
ShahAlam	Malaysia	60 (0-130)	40 (0-110)	70 (10-150)	70 (10-150)	70 (10-150)	60 (0-140)	60 (0-130)
Pasig	Philippines	0 (0-0)	0 (0-0)	0 (0-0)	0 (0-0)	0 (0-0)	0 (0-0)	0 (0-0)
Balikpapan	Indonesia	0 (0-0)	0 (0-0)	0 (0-0)	0 (0-0)	0 (0-0)	0 (0-0)	0 (0-0)
Serang	Indonesia	50 (10-90)	50 (10-90)	50 (10-90)	50 (10-90)	50 (10-90)	50 (10-90)	50 (10-90)
PetalingJaya	Malaysia	60 (0-120)	40 (0-110)	70 (10-140)	70 (10-140)	70 (10-140)	60 (0-130)	60 (0-130)
Kuching	Malaysia	50 (0-100)	0 (0-0)	50 (0-110)	0 (0-0)	50 (10-130)	0 (0-60)	0 (0-0)

1036 Figure 6. Premature mortality in different years from 2002 to 2008 and cities in Association of
1037 Southeast Asian Nations (ASEAN) due to exposures PM_{2.5} in FFBB (95% confidence intervals).
1038 Colors from green to red represent relative number scale.
1039





1040

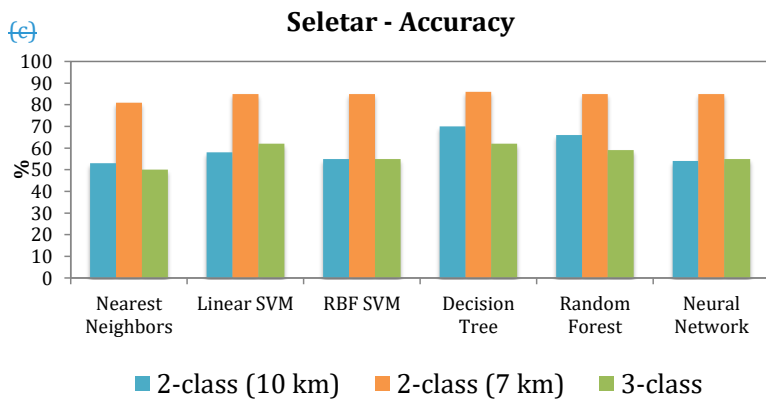
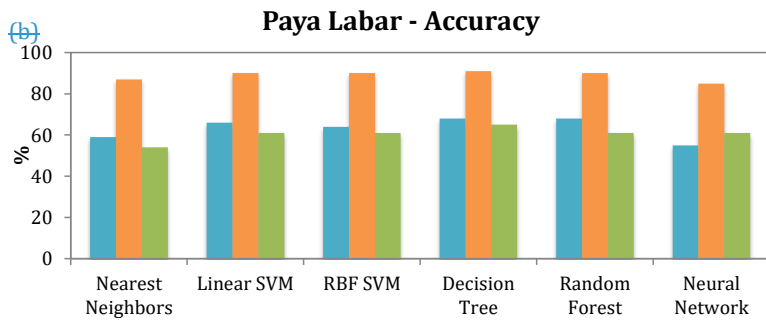
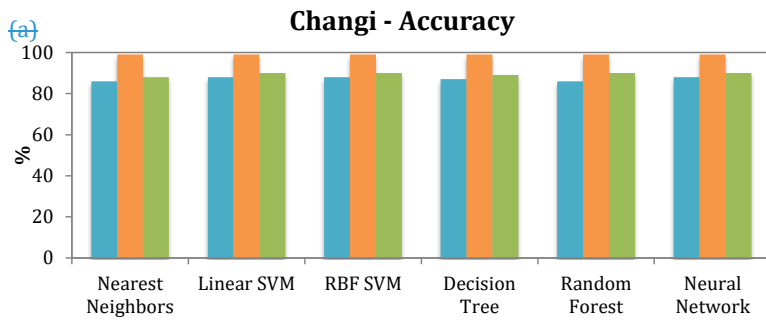
1041 Figure 7. Total monthly mean precipitation differences (mm day^{-1}) between FFBB and FF
 1042 simulations during 2002–2008. Black dot indicates differences that are statistically significant at
 1043 a significance level of $\alpha_{\text{fdr}} = 0.05$ after controlling the false discovery rate (FDR) (Benjamini
 1044 and Hochberg, 1995; Wilks, 2016). The two tailed p values are generated by Welch's t test,
 1045 using monthly mean data as the input. The approximate p value threshold, p_{fdr} , and area mean
 1046 and standard deviation (over land only) are written in above the map.

1047

1048

1049

1050



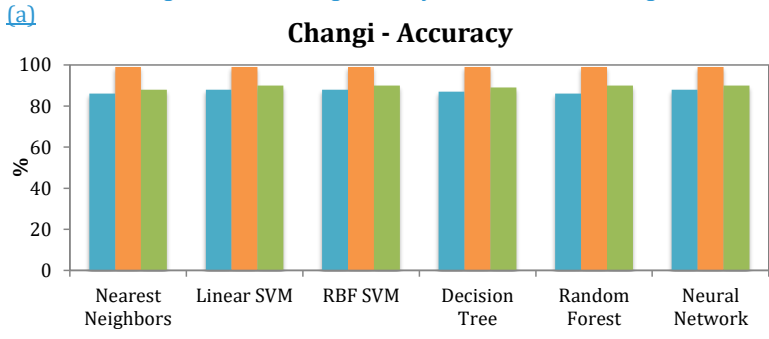
1051

1052

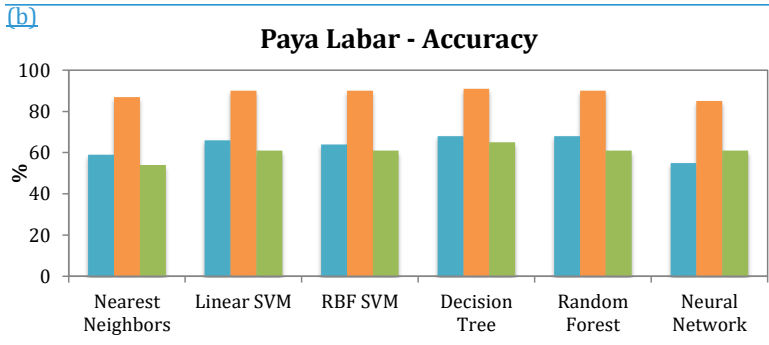
1053

1054

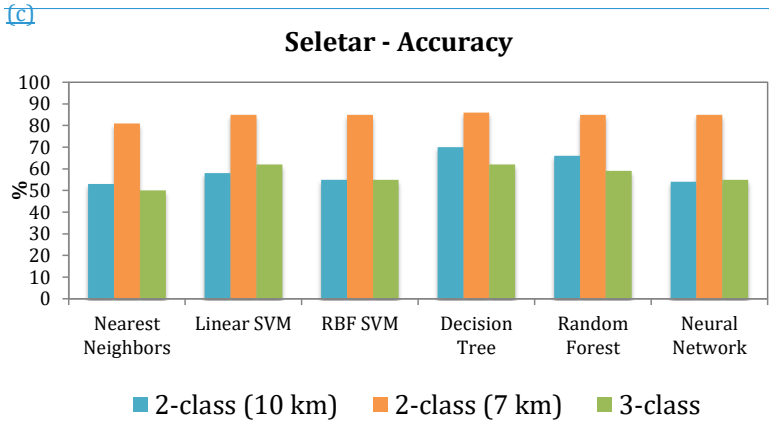
Figure 8. The testing accuracy in 6 Machine Learning



1055



1056



1057

1058

1059

1060

1061

Figure 7. The testing accuracy in 6 machine learning algorithms for two 2-class (7 km or 10 km visibility as a breakpoint) and one 3-class classifications haze prediction in (a) Changi, (b) Paya Labar, and (c) Seletar. The units are in percentage.

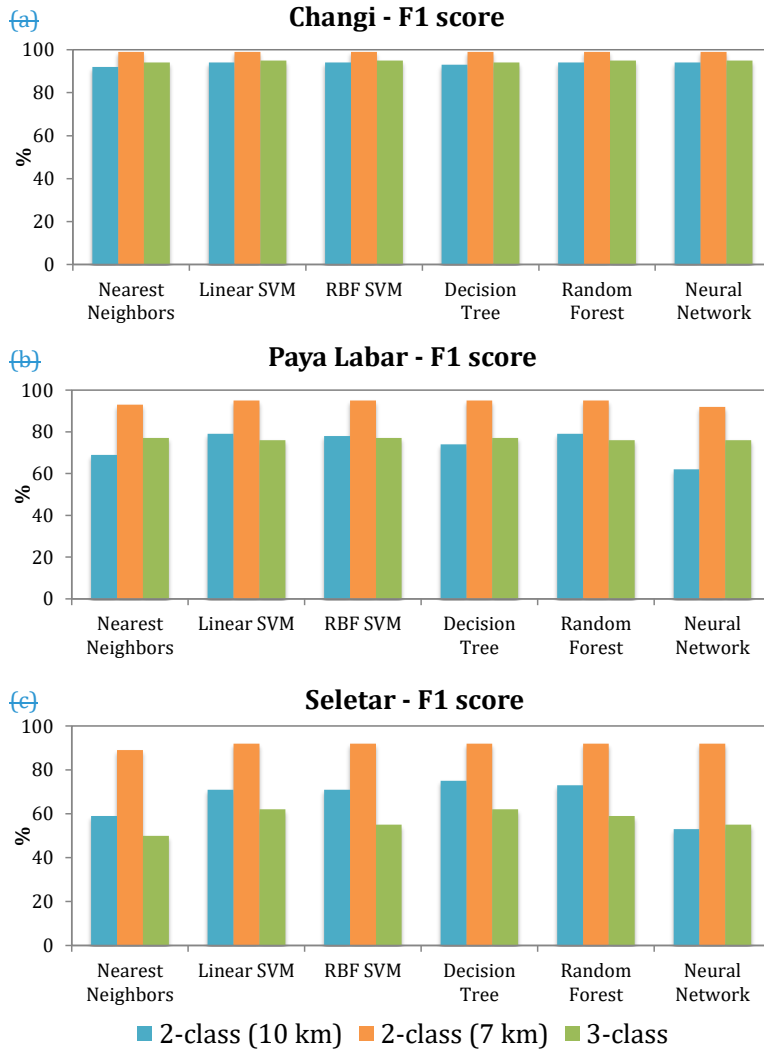
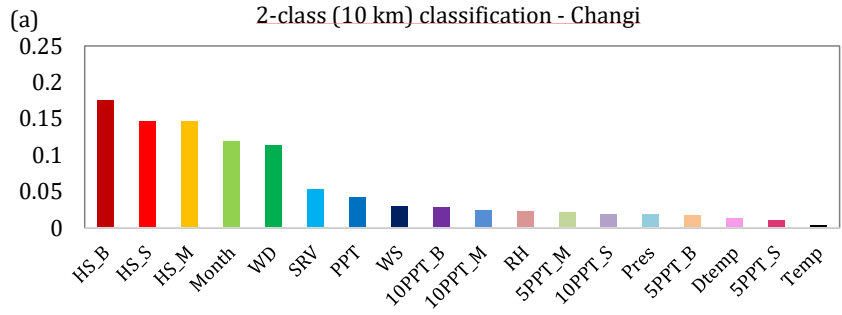
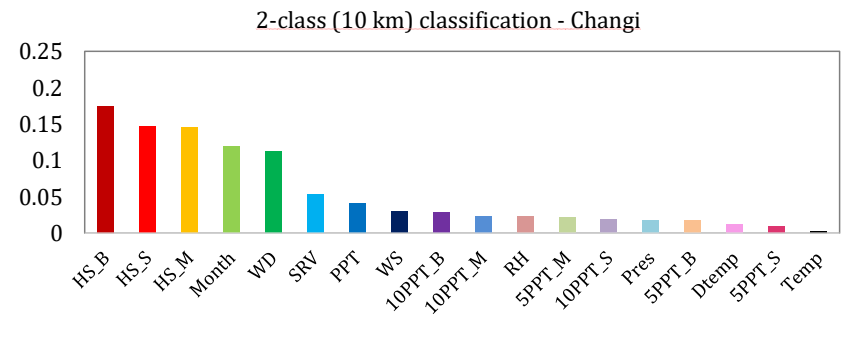


Figure 9. The F₁ score in 6 Machine Learning algorithms for two 2-class (7 km or 10 km visibility as a breakpoint) and one 3-class classifications haze prediction in (a) Changi, (b) Paya Labar, and (c) Seletar. The units are in percentage.

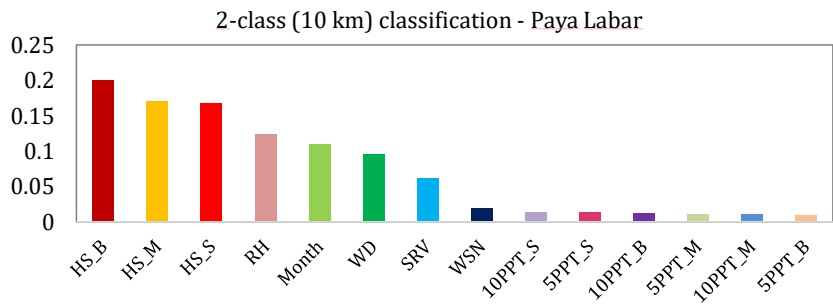
1070



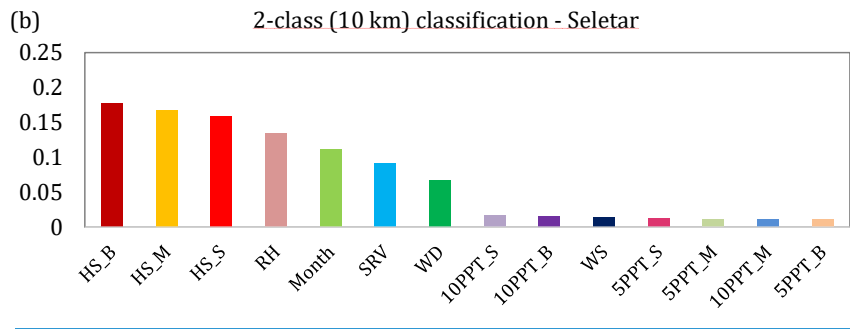
1071



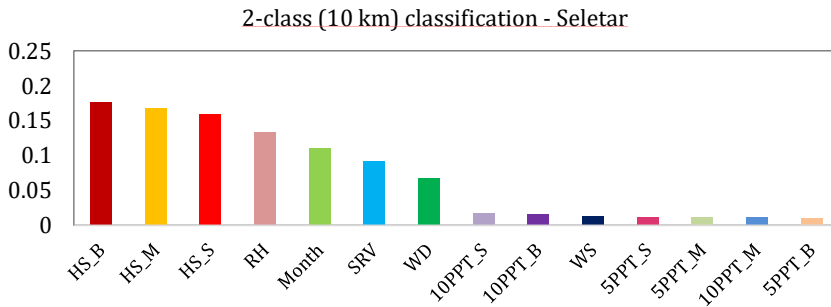
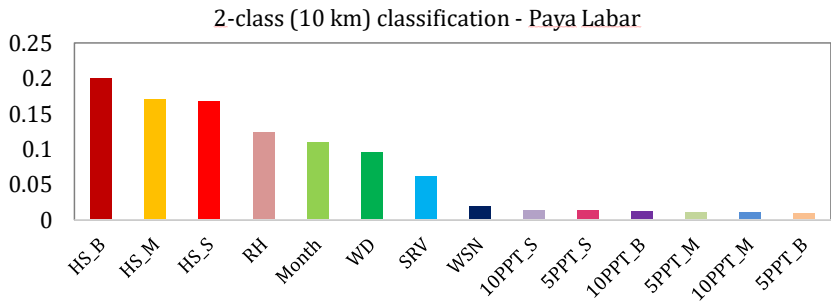
1072



1073



(c)



1074

1075

1076

1077

1078 Figure 408. Feature importance by using 2-class classification Random Forest algorithm in (a)
 1079 Changi, (b) Paya Labar, and (c) Seletar. Desired outputs, haze versus non-haze events, are
 1080 defined by using visibility 10 km as a breakpoint. Full name of each input feature are listed in
 1081 Table S3S5.

1082

1083

1084 [Benjamini, Y., and Hochberg, Y.: Controlling the False Discovery Rate: A Practical and
 1085 Powerful Approach to Multiple Testing, Journal of the Royal Statistical Society. Series B
 1086 \(Methodological\), 57, 289-300, 1995.](#)

1087 [Wilks, D. S.: "The Stippling Shows Statistically Significant Grid Points": How Research
 1088 Results are Routinely Overstated and Overinterpreted, and What to Do about It, Bulletin of
 1089 the American Meteorological Society, 97, 2263-2273, 10.1175/BAMS-D-15-00267.1, 2016.](#)

1090

1091